Effects of Cu-Doping on PbS Thin Films

A thesis submitted

In partial fulfilment of requirements for the award of degree of

Masters of Sciences

In

Physics

Submitted by

Keerti Bector

Reg. No. 301304004

Under the guidance of

Dr. Bhaskar Chandra Mohanty

School of Physics and Material Science

School of Physics and Material Science

Thapar University

(Established under section 3 UGC act, 1956)

Patiala -147001, India

CERTIFICATE

This is certify to that thesis entitled "**Effects of Cu- doping on PbS thin films**" submitted by Neetu Bector, **Roll no. 301304004** in partial fulfilment of requirements for the award of the degree M.Sc. in **Physics** from the School of Physics and Material Science, Thapar university, Patiala, is a record of candidate's own work carried out by her under my supervision and guidance. The matter embodied in this report has not been submitted in part or full to any other university or institute for award of any degree.

17/7/2015

(Dr. B.C. Mohanty)
Assistant professor
School of Physics and Material Science
Thapar University, Patiala-147004(Punjab)

Countersigned by

(Dr. Manoj Sharma)
Professor & head
School of Physics and Material Science
Patiala-147001(Punjab)

(Dr. S.S. Bhatia)
Dean of academic Affairs
Thapar University
Patiala 147001(Punjab)

Dated:

DECLARATION

I hereby declare that the work being presented in this thesis report entitled "**Effect of Cu doping on PbS thin films**" by me in partial fulfilment of the requirements for the award of degree of **Masters of Science** in **Physics,** Thapar university Patiala is an authentic record on my work carried out under the supervision of **Dr. Bhaskar Chandra Mohanty,** Assistant Professor, school of physics and material science, Thapar university. The matter presented in this report has not been submitted in any other university/institute for award of masters of Sciences or any other degree.

Keerti Bector

Keerti Bector

Reg. No.301304004

ACKNOWLEDGEMENTS

I would like to express my deep sense of gratitude to Dr. B.C. Mohanty, Assistant professor School of physics and material science, Thapar University, Patiala for his invaluable suggestion, excellent supervision, constant encouragement, thought provoking and unabashed discussion in nurturing the work and during the preparation of manuscript throughout the research work.

My sincere thanks to Dr. Manoj Sharma, professor and head of school of physics and material Science, Thapar university, Patiala and Dr. S.S. Bhatia, dean of academic affairs, Thapar university Patiala for providing me with the opportunity to conduct this work and bring it out in the present form.

I offer special thanks and regards to Ms. Indu Gupta, Ms Parveen Kaur, Mr. Satwinder Singh, Mrs Sakshi Gupta, research Scholars, School of Physics and Material Science, Thapar University, Patiala for providing immense support in performing, characterizing and evaluating the thesis work.

I would also like to thank my friends (Rahul Goyal, Bharti Chugh, Pritampal Singh and Shilakha Dawar) for their kind support and encouragement.

The greatest thanks go to my family members for their infinite support at each and every part of my life. Above all, I express my indebtness to the almighty for all his blessing and kindness.

ABSTRACT

Cu-doped PbS thin films were grown on glass substrates by a simple and expensive technique, namely the chemical bath deposition process (CBD) at a bath temperature of 60 °C. Lead acetate, thiourea and copper chloride were used in aqueous solution as ion sources of Pb, S and Cu, respectively. All films were synthesized in a single step by dipping the substrates in the bath solution. The deposition time was varied from 2 to 30 min to investigate the evolution of the properties. The properties of resulting thin films were characterised by various techniques such as X- ray diffraction (XRD), field emission scanning electron microscope (FE- SEM) and UV-visible spectroscopy. It was found that for the undoped films, no deposition was possible up to a deposition time of 5 min. When the substrates were dipped for longer durations, the growth of the films proceeded from heterogeneous nucleation of crystallites followed by their coalescence. The films were found to be discontinuous for deposition times as long as 30 min. In contrast, the doped films showed a continuous film with surface covered by crystallites whose size and shape continuously decreased with the increase in Cu concentration. The continuous nature of the film is attributed to the formation of the initial layer of Cu_7S_4, as revealed from the XRD analysis, on which further growth of the films proceeded. For the undoped films, the transmittance remained relatively higher compared to the doped samples because of the discontinuous nature of the undoped films. However, with increase in deposition time, the transmittance decreased gradually due to the increased surface coverage of the glass substrates. For all the doped films, the transmittance gradually decreased with increasing deposition time due to higher absorption of incident photons. For small concentration of Cu up to 5%, the band gap marginally decreased and then, continuously increased from about 1.40 eV for 5% Cu doping to about 1.76 eV for 20% Cu-doping. Based on these results, it is believed that Cu-doped PbS thin films grown by the CBD process can be a potential candidate for PV applications.

CONTENTS

LIST OF FIGURES

CHAPTER 1
INTRODUCTION

Thin solid films exist as crystalline or non-crystalline solid materials grown upon two dimensional substrate surfaces. From the technological point of view the miniaturization of devices with specific electronic, optical and optoelectronic properties depends on surface to volume ratio of the materials. Nonetheless, the surface properties are different from the bulk properties which banks on the number of atoms with in the material [1].

Thin films can be found in optoelectronic, electronic and magnetic components which are manufactured based on the special physical properties of these films and as mentioned above, the associated properties may different be from those of the bulk material. This has been capitalized to technological advantage, and consequently, thin films have been widely studied, both theoretically and experimentally through the years. They have also been adapted to fulfil a wide variety of functions and have been used in applications as diverse as electronics, energy harvesting systems, corrosion resistance and protection, bio-mechanics, magnetic coatings, decoration and data storage, etc. [2].

In the recent years, thin films are being freely studied for their potential applications in photovoltaic (PV) technology. The PV has materialized as an alternate key technology following the serious environmental threats for energy solutions of the human race. The PV technology engages solar cells and modules which turns sunlight directly into electricity. The sun light is copious, freebie, and cannot be monopolized by a single nation, and seems to have a vivid future. Interestingly, the PV technology industry has savoured a stupendous yearly growth rate averaging nearly 40 % in the past decade. Despite overwhelming acceptance of the PV technology and a forecast of $100 billion business by 2020, the PV energy is high priced than that from the fossil fuel technologies. Henceforth, it has become imperative to identify courses for the curtailment of cost, which can be achieved by several methods such as better materials management, development of cost effective production processes and new techniques to amplify the existing solar cell efficiencies [3].

Binary sulphide based thin film solar cells

Metal sulfides (MS) have drawn much attention over the last few years owing to their unique optical properties, as well as multiple prospective applications in photovoltaic devices, light-emitting devices and photo detectors, etc. The MS thin films exhibit highly tuneable

optical properties, which is highly useful for various applications [4]. Especially, the band gap of the MS thin films have been shown to vary with considerable ease. Current high-efficiency absorber layers in thin-film photovoltaic (PV) cells, such as copper indium gallium sulfide/selenide (CIGS) and cadmium telluride (CdTe), Cu_2ZnSnS_4 bank on low-abundance elements and thus are envisioned to face supply shortages in the long haul. In response to this forewarn, interest in Cu_2ZnSnS_4 (CZTS) and $Cu_2ZnSn(S,Se)_4$ (CZTSSe) as sustainable alternatives to CIGS has been proliferating. On the other hand, a large work function wide band gap and high transmittance have made *n*-type sulphide thin films very attractive for use in efficient solar cell. A number of binary sulfides are being examined as a possible absorber layers in thin film solar cells grown through cost-competitive techniques. More recently, p-type PbS and n-type CdS thin films have drawn significant interest for their properties suitable for PV applications [5-6].

Properties of PbS thin films

Structural properties

PbS crystallizes in the rock salt structure with a lattice parameter of about 5.93 Å. **Figure 1.1** shows a unit cell of PbS in the rock-salt structure. In quintessential configuration, each Pb atom has six S neighbouring atoms, which are arranged at the corners of an octahedron. Each S atom is surrounded by six Pb atoms at the corners of octahedron as shown in the figure below [7].

The nature of bonds between PbS and S has been extensively studied. Some regard this bonding as ionic, other covalent and still other, concoction of both ionic and covalent. But ionic bonding is reckoned more important because ionic character dwindles as the size of S species increases [8].

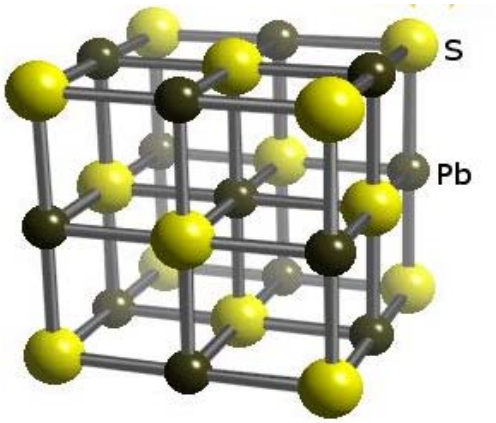

Fig. 1.1: Typical structure of PbS (cubic)

Optical properties:

When a film is illuminated by a light source of photon flux Φ_o with photon energy hν greater than the band gap (E_g), the fraction of the photons absorbed is proportional to the intensity of the flux [9]. Therefore, the number of photons absorbed with in distance *d* is given as:

$$\Phi\ (d) = \Phi_o\ e^{-\alpha d}$$

Where α is the absorption coefficient and *d* is the film thickness. The negative sign indicates decreasing intensity of the photon flux due to absorption. Various experimental results have indicated that the bulk PbS has a very narrow band gap of ~ 0.4 eV [10]. However, this value can be raised to the order of 2 eV, when the crystallite size of PbS decreases. Owing to rather a large Bohr radius, PbS exhibits strong quantum confinement effects. The processing parameters which greatly affect the morphology and particle size of the films eventually control the optical absorption and the band gap of the films [11].

Photoconductivity:

Photoconductivity is a phenomenon where a material shows better electrical conductivity under irradiation of electromagnetic waves of appropriate wavelength. This is observed in nearly all of the semiconductors. The opto-electric properties can also be severely affected by concentration of impurities or any other lattice defects causing indented fluctuations of the electric potential [12-13]. The photosensitivity of PbS films has a dependence on the surface morphology. [14-15]. It has been shown that the photo-response depends on crystallite size and the morphology of the film; i.e. on the uniformity of the crystallite size distribution and degree of compaction of the formed structure.

Deposition of PbS thin films

There have been primarily two methods, namely physical and chemical methods. The physical methods involve expensive tools and high vacuum to deposit the films. On the other hand, the chemical methods such as electrolytic deposition, anodic deposition, chemical vapour deposition, chemical bath deposition (CBD), etc. are simple and inexpensive. Hence, over the years, the chemical methods have used to prepare not only the PbS films but also many of the binary sulphides [16]. Among all, the CBD technique that has the advantages of being simple, inexpensive and offers the possibility to deposit on large area substrates has drawn significant interest. In fact, CBD is the most preferred technique for growth of binary sulphide thin film

and the PbS was first film prepared by the CBD technique [17]. **Figure 1.2** shows the setup of the CBD technique. In CBD, a substrate is dipped into chemical bath solution for the growth of film for specific period of time. We require precursors for the solution and chalcogenide source as a reaction source. Basically, CBD technique relies on the precursors and growth parameters. CBD mechanism can happen by four ways exemplified as follows [18].

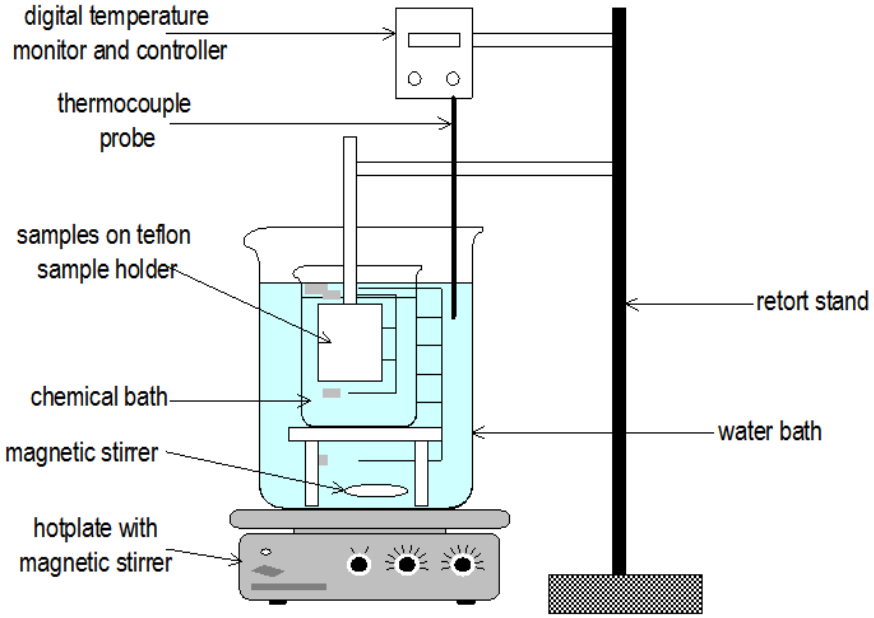

Fig 1.2 A setup for film deposition using CBD process

Mechanism of the CBD process

There are four ways by which the growth of the films in the CBD technique can proceed and have been briefly described below.

1. Ion by ion mechanism
2. Hydroxide cluster mechanism
3. Complex decomposition mechanism
4. Cluster mechanism

1. Ion-by-Ion Mechanism

The ion-by-ion mechanism is the simplest mechanism, and occurs by sequential ionic reactions. The principle of this mechanism is explained with the example of CdS, and is given by

$$Cd^{2+} + S^{2-} \rightarrow CdS$$

If the ion product $[Cd^{2+}][S^{2-}]$ transcends the solubility product, K_{sp}, of CdS, then CdS turns into a solid phase.

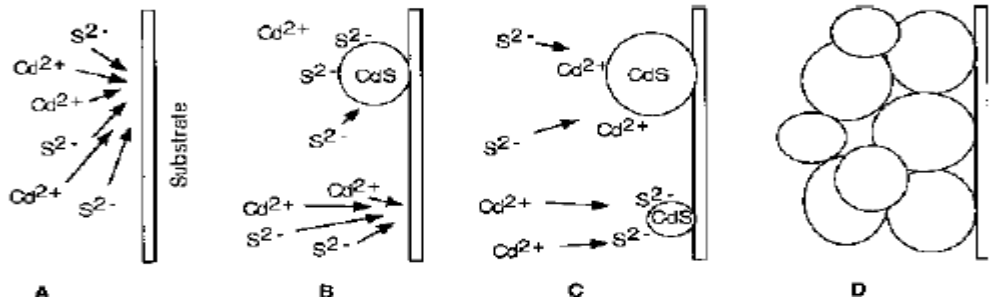

Fig. 1.3: schematic diagram indicating various steps in the ion-by-ion mechanism. a: diffusion of ions to the substrate, b: nucleation of the ions to form the compound nuclei, c: growth of CdS nuclei by adsorption of cd and s ions from solution and nucleation of new CdS crystals, d: continued growth of CdS crystals.

2. Hydroxide Cluster Mechanism

Usually during the CBD process, complexation of the Cd was necessary to fortify $Cd(OH)_2$ precipitation, which would impede the growth of CdS thin films. The CdS is then formed by reaction of slowly generated S^{2-} ion with the $Cd(OH)_2$:

$$Cd^{2+} + 2OH^- \rightarrow Cd(OH)_2$$

Followed by $$Cd(OH)_2 + S^{2-} \rightarrow CdS + 2OH^-$$

In this case, sulfide formation will occur preferentially at the surface of the hydroxide rather than nucleate separately in the solution. This reaction occurs both at the surface-adsorbed colloids and at those dispersed in the solution. The reaction continues till all of the hydroxides get conversted into sulfides. Finally, these sulfide particles adhere to each other and grow to form the continuous sulfide film on the substrate.

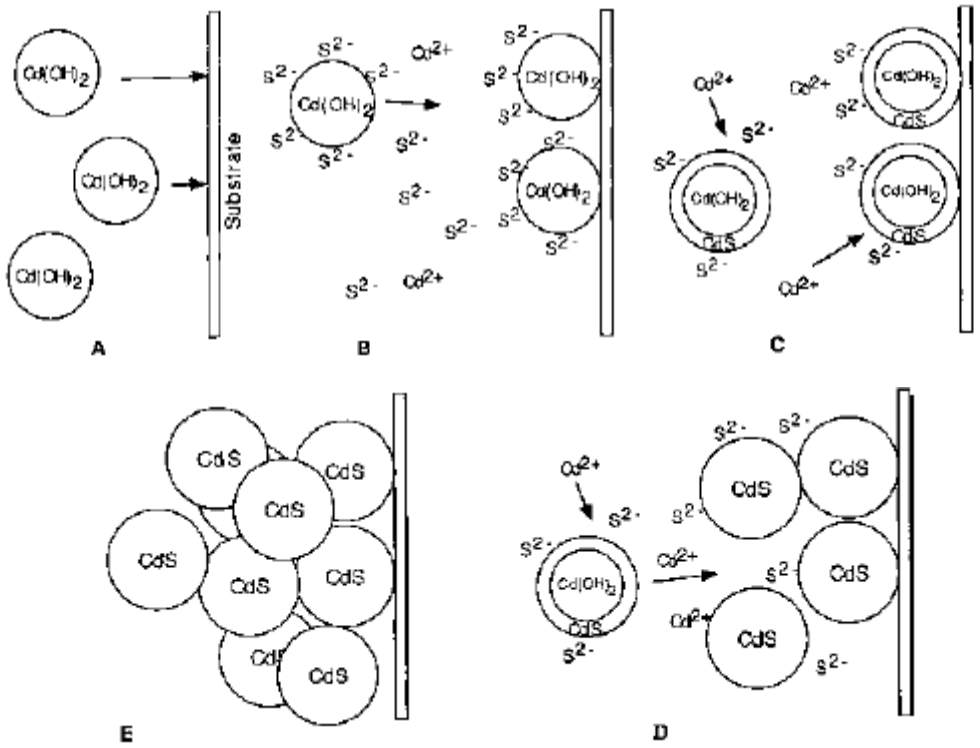

Fig. 1. 4: A: Diffusion of hydroxide colloidal particles & adherence to substrate, and (B) react with S ions. This reaction start at the surface of the colloid (on surface and inside solution) and proceeds inward (C). Reaction continues till all hydroxide is converted to sulphide (D); Particles of CdS will adhere to each other to form an aggregated film (E)

3. Complex-Decomposition Mechanism

This mechanism has been proposed in the cases of strong complexation between the chalcogen compound and the metal ion (e.g., as occurs between thiosulphate and Hg, Ag, and Cu). The weak secondary bond is thought to break easily than the very strong metal - chalcogen bond. Hence, the chemically complex species that contains both metal and sulfur will decompose to form the binary sulfide, as illustrated in **Fig. 1.5**.

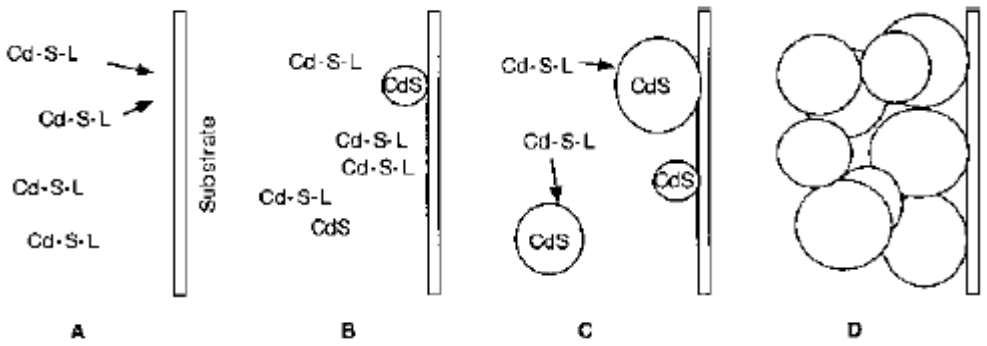

Fig. 1.5: The complex (Cd-S-L, where L is a ligand or part of the S-forming species) decomposes to CdS on the substrate and also homogeneously in the solution (A, B). The CdS nuclei formed grow by adsorption and decomposition of more complex species (C) until a film of aggregated crystals is formed (D) in the same manner as for the previous two mechanisms.

4. Cluster Mechanism

In this mechanism, the free anion does not react directly, in fact a solid phase is formed and it forms an intermediate complex with the "anion forming" reagent. For the example of CdS, this would be given as

$$Cd(OH)_2 + (NH_2)_2CS \rightarrow\leftarrow Cd(OH)_2 . SC(NH_2)_2$$

Where $Cd(OH)_2$ is one molecule in the solid-phase cluster. This complex or a similar one containing also ammine ligands, then decomposes to CdS:

$$Cd(OH)_2 . SC(NH_2)_2 \rightarrow CdS + CN_2H_2 + 2H_2O$$

i.e., the S-C bond of the thiourea breaks, leaving the S bound to Cd [19].

CBD PbS thin films

A number of studies have been done on the growth of Cu doped PbS thin films by the CBD process. It has been found that the deposition time, bath temperature, concentration, doping and pH are the most important parameters by which properties of films are influenced. Many researchers have been studying the influence of these parameters to obtain films of desired properties. The summary of some researchers work is listed below.

Preetha et al. have deposited PbS thin films by successive ionic layer absorption and reaction (SILAR) method on soda lime glass substrate.They have used lead acetate, lead nitrate, lead chloride or lead sulphate as source of cation and thioacetamine as source of anion respectively. They showed that the size of crystallites depended on the cationic sources, and it affected the structural, optical and morphological properties of PbS thin films [20]. Gode et al.

deposited PbS thin films on glass substrate by the CBD process. The variation in deposition time at room temperature decreased the band gap from 2.65 to 2.50 eV. The electrical conductivity increased from 1.791×10^{-6} to 1.655×10^{-3} Ω.m with increase in the deposition time [21]. Nair et al. have deposited PbS thin films and showed increased rate of deposition under sunlight or other sources of illumination effects photo thermal conversion as well as of photo activated deposition on the PbS film [22]. Raniero et al. focused on deposition of PbS thin films using an aqueous solution of lead nitrate, sodium hydroxide and thiourea for 30 minutes by CBD process [23]. Altıokka et al. deposited polycrystalline PbS thin films using lead nitrate, sodium hydroxide, thiourea and sodium sulfide in the final solution was determined to be 0.0089, 0.1460, 0.510 and 0.00023 M respectively on glass substrates at 303 K using the CBD technique. The precipitation of PbS on solid surfaces was performed using the sodium sulfide compound. It was found that the precipitation rate effects the formation of pinhole. The XRD results showed that the films formed galena cubic structures [24]. Ileana pop et al. investigated chemically deposited thin films from alkaline bath solution using lead nitrate, thiourea, triethanolamine or H_2O_2 which showed photosensitivity as thickness varied from 0.12-0.54 μm [25].

Valuenzula et al. have deposited PbS thin films by CBD process at different bath temperatures 10, 15, 20, 25, 30 ºC. The thickness, void fraction and roughness of films were changed with the variation in temperature [26]. Abbsa et al. prepared nanostructure PbS thin films by CBD process where the optical and structural properties shows influence with the increase of thickness. The XRD results showed that the grain size increases with the increase of film thickness. The value of band gap varied from 2.31 to 2.19 with the increase of thickness [27]. Valuenzula et al. synsthesized lead sulfide thin films using Pb (CH_3COO_2), NaoH, (NH_2)CS, $N(CH_2CH_2OH)_3$ and CH_3CH_2OH in aqueous solution on glass substrate by chemical bath deposition. It has been observed that the increase in deposition time increases the film thickness, crystallite size and decrease in the energy band gap. The film deposited for 4 hour presented thickness 181 nm; crystallite size 13.8 nm and energy band gap 0.93 eV [28].

Tohidi et al. synthesized high quality PbS thin films on glass substrate from two different baths compositions. One of them (bath-I) contained an aqueous solution of lead acetate, thiourea, sodium hydroxide, and the second (bath-II) had additional triethanolamine. The introduction of triethanolamine in second bath solution reduced the grain size and increased the optical band gap of the PbS nanoparticles [29]. Patil et al. deposited PbS thin films on glass substrates from the solution containing 0.1M lead nitrate, 0.1M thiourea. The pH of solution is maintained at 9 and temperature at 300 K. Despite a longer deposition time

of 2 to 7 hours, the films had very small crystallites of dimensions of a few nanometres. The films exhibited p-type conductivity of order of 10^{-4} $(\Omega cm)^{-1}$ [30]. More recently, Obaid et al. have synthesized Nano crystalline PbS thin films on glass substrates from solutions composed of 0.1M lead nitrate and 0.1M thiourea dissolved in distilled water. Deposition time was varied ranging from 30 to 120 minutes. Atomic force microscopy (AFM) images confirmed that particles were of nano size and surface roughness increased with the increase in deposition time [31]. Huang et al. prepared Quantum dot sensitized solar cells of PbS with Cu doping using (SILAR) method in which Cu-concentration was varied by adding appropriate amount. The $CuCl_2$ to $Pb(NO_3)_2$ (0.1 M) in an ethanol and deionized water (1:1) mixed solution as cation source, respectively and Na_2S (0.1M) in methanol was used as anion source. A solar cell conversion efficiency of 2.01% was achieved with Cu-doped-PbS/CdS quantum dot-sensitized solar cell. The absorbing ability of PbS of incident photons is enhanced by Cu doping [32]. Merino et al. prepared Cu doped PbS Nano crystalline films from CBD at temperature of 80 °C on glass substrates. Different Cu concentrations were used for the growth of PbS in the solution. The grain size determined by XRD of the undoped samples, was found 37 nm, whereas for the doped sample was 32–25 nm. Raman spectra of the films showed a strong band in 133–140 cm^{-1}. Optical absorption, forbidden band gap energy (Eg) was found in the range 1.4–2.4 eV [33].

Motivation and objectives

As the brief literature review presented above indicates, there has been a very limited study of effects of Cu doping in PbS thin films grown by CBD. We envisage that Cu doping by an appropriate amount can significantly affect the optical and electrical properties of the PbS thin films and render it more suitable for the PV applications.

The main objectives of the present work can be summarised as following:

- Growth of Cu doped PbS thin films by a simple and inexpensive technique such as CBD
- Study of effects of Cu doping on structural and optical properties of PbS thin films.
- Investigation of evolution of properties of CBD Cu-doped PbS thin films at a given bath temp (at 60 ºC).

CHAPTER 2

EXPERIMENTAL TECHNIQUES

In this chapter, experimental techniques used for the growth and characterization of Cu-doped PbS thin films are presented. Section 2.1 gives the brief description of thin film preparation; the techniques used for the characterization of films are presented in section 2.2.

2.1 Growth of PbS thin films

There have been a variety of methods reported in literature to prepare the binary sulfide thin films that includes vacuum techniques such as thermal evaporation and sputtering, etc., spray pyrolysis , chemical vapour deposition , and many solution processes [34-38]. Amongst all, the CBD process is the most attractive method to grow the films due to easy control of parameters, ability to prepare the films at relatively low temperatures on large area substrates [39].

In this work, lead acetate ($Pb(CH_3COO)_2.\ 3H_2O$) and thiourea ($NH_2.CS.NH_2$) were used as sources for Pb and S in the CBD process. Stock solutions of 10 ml of 0.5M lead acetate, 12 ml of 1M of thiourea, 10 ml of 2M NaOH and 8 ml of 1M triethanolamine were prepared in distilled water. **Fig 2.1** shows the photographs of prepared stock solutions. The total volume of the deposition bath was made 400 cm^3 by adding DI water. The reagents namely $Pb(CH_3COO)_2$, TEA and NaoH were added under constant stirring. The glass slides were firstly washed with detergent solution, followed by ultrasonic cleaning with DI water and acetone for 10 min each. The cleaned glass slides were kept vertically in the solution. After inserting the glass slides, thiourea solution was added under constant stirring. In typical conditions, only one substrate was used. Stirring of the solution was carried out at a speed of about 1000 RPM for the entire duration of deposition (from starting to end till the substrates removed from solution). All films were made in single step. To study the evolution of film properties, films were grown for various deviations in ranging from 2 to 30 minutes. After the injection of thiourea, the colour of the solution slowly changed to black. The rate of change of colour depended on the deposition time. **Fig 2.2** shows the photographs depicting of colour of the solution. For temperature measurement, a thermometer (with an accuracy of ± 1 °C) was dipped inside the solution for the whole period of deposition. After the specified period of time, the deposited thin films were removed from the solution and were ultrasonically cleaned in deionised water. followed by air drying.

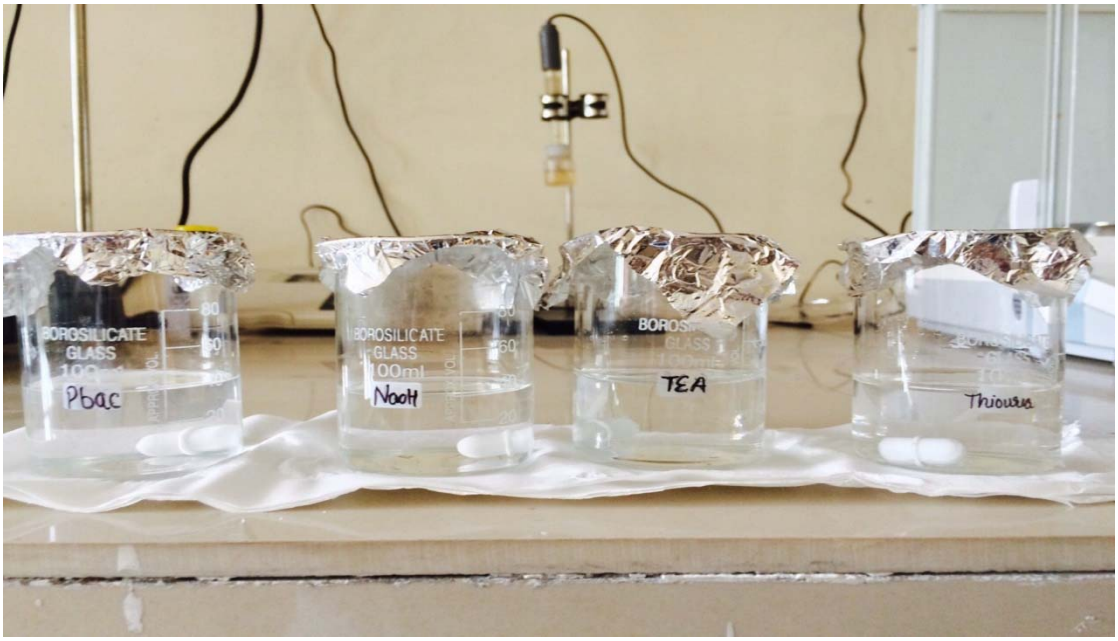

Fig. 2.1: Photographs of the prepared stock solutions of lead acetate, NaOH, triethanolamine and thiourea.

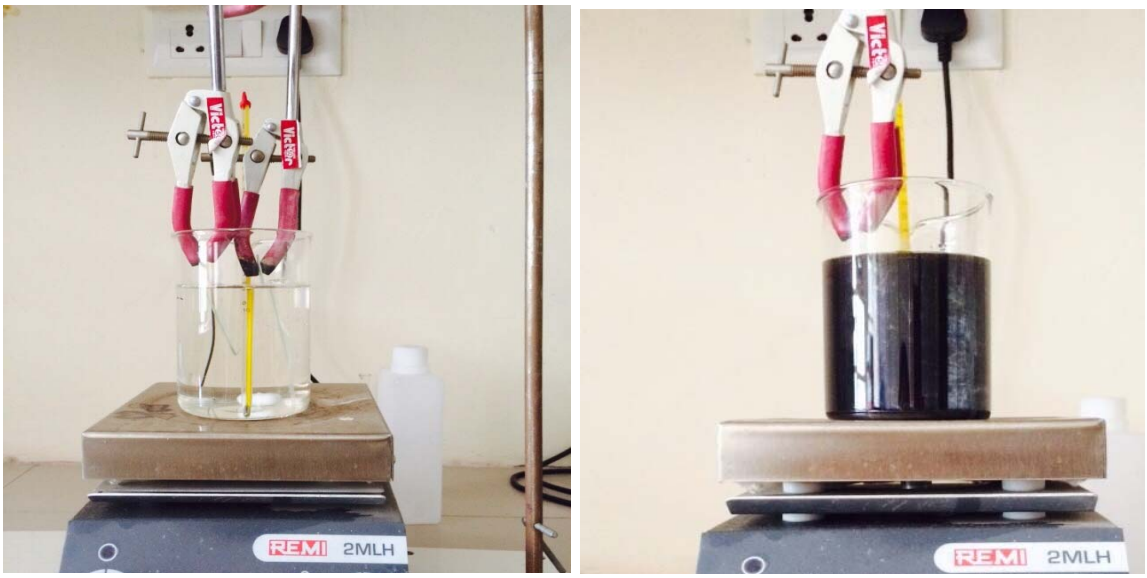

(a) (b)

Fig 2.2: The colour of the bath solution changes with time. The photograph (b) was taken after 30 minutes from starting of deposition.

For Cu doping of the films, appropriate amounts of the copper chloride (CuCl2.2H2O) was added to the solution. The depositions process remained the same. In this work the % copper doping was in the range from 1 to 20 mole %. The bath temperature was 60ºC.

2.2 Characterization Techniques

2.2.1 Structural characterization using X-ray diffraction (XRD)

For any type of crystalline material, XRD analysis allows the determination of phase purity, structure, crystallite size and strain [40]. As the technique employs, X-rays are electromagnetic waves whose wavelengths are of order of few angstroms. When parallel beam of X- ray is allowed to strike on a crystalline material, they are scattered at different angles according to the periodic nature of atomic arrangement in the crystalline material. Thus, we get a diffraction pattern of peaks of substantial intensity at specific angles.

Fig. 2.3 depicts the principle of X-ray scattering by rows of atoms. Bragg's formula gives the information of lattice spacing (d_{hkl}) using relation,

$$\mathbf{2d_{hkl}\ Sin\theta = n\lambda} \qquad \text{..... (2.1)}$$

Where 2θ is the corresponding Bragg's angle, n is the order of diffraction and λ is the wavelength of the X-ray**.**

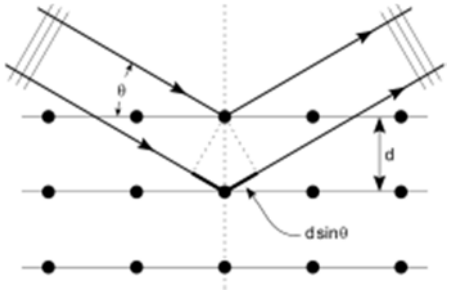

Fig.2.3: Diffraction of X-ray by planes of atoms

In the present work, the measurement of undoped PbS thin films were carried out in a PAN analytical (model: X Pert PRO) XRD unit using Cu-Kα radiation in the conventional θ-2θ mode. By comparing the data with established JCPDS data, the phases of the films were identified and the peaks in the patterns were indexed.

2.2.2 Surface microstructure studies

Surface and cross sectional microstructure of the films were studied by field emission scanning electron microscopy (FE-SEM). There are excellent books which deal with the study of surface morphology [41-45]. A brief account of this technique is given in the following section.

2.2.2.1 FE- SEM

FESEM allows the imaging of surfaces using electrons instead of visible light. These electrons are liberated by a field emission source. FESEM has advantages of greater magnification and much greater depth of field. When a fine focussed beam of electrons is passed across the sample surface, it generates secondary electrons, backscattered electrons and characteristic X-rays. These secondary electrons are responsible to form an image of the surface because of the inelastic interaction between the incident electron beam and the electrons in the sample. Backscattered electrons generated due to elastic interaction between incident electrons and the sample electrons give the contrast based images based on atomic number to resolve composition variations, as well. However, the surface features are not resolved properly since backscattered electrons can escape from deep within the sample due to their high energy. The emission of X-rays analysis gives the qualitative and quantitative chemical information.

The SEM measurements were carried out on the films using ZEISS (model) field emission scanning electron microscope. Some cross sectional images of selected samples were also taken. The operating voltage used during the measurements was of 15 KV.

2.2.3 Optical transmittance and band gap measurement

The properties of thin films like optical transmittance, absorbance and band gap make them suitable for photovoltaic applications. UV-visible-NIR spectroscopy is used for evaluation of these properties. The UV-visible-NIR spectroscopy is based on the principle that, when light passes through a material, its intensity decreases exponentially. This is expressed through the Beer-Lambert law:

$$I = I_0 e^{-\alpha d} \quad \text{..... (2.2)}$$

Where I_0 is the intensity of the incident light on the sample, α is the absorption coefficient and *d* is the thickness of the sample. Rearrangement of Eq. (2.2) gives

$$\alpha = -\frac{1}{d}\ln\frac{I}{I_0} \quad \text{..... (2.3)}$$

Often the ratio I/ I_0 is transmittance (T) of the sample. Hence, the absorption coefficient (α) and the transmittance (T) of the film are interrelated through the equation

$$\alpha = -\frac{1}{d}\ln T \quad \text{..... (2.4)}$$

One can estimate the value of fundamental absorption edge (band gap) by plotting $(\alpha h\upsilon)^2$ as function of hυ, by following the given relation of direct allowed transition,

$$\alpha = \frac{A_1}{h\upsilon\,(h\upsilon - Eg)^{1/2}} \quad \text{..... (2.5)}$$

Where A_1 is a constant and E_g is the energy gap. If we plot the graph of $(\alpha h\upsilon)^2$ vs $h\upsilon$, the extrapolated intercept on the abscissa gives the value of E_g. This method is helpful for determining the band gaps of semiconducting thin films [46-49].

Light source, a sample holder, a monochromators and a detector are the main components of spectrophotometer. The detector is basically a photomultiplier tube, a photodiode, a photodiode array or a charge coupled device (CCD). To filter the light so that only light of a single wavelength reaches the detector at one time single photodiode detectors and photomultiplier tubes are used with scanning monochromators. Fixed monochromators are used with CCDs and photodiode arrays. When many detectors grouped into one or two dimensional arrays, then they become able to collect light of different wavelengths on different pixels or groups of pixels simultaneously.

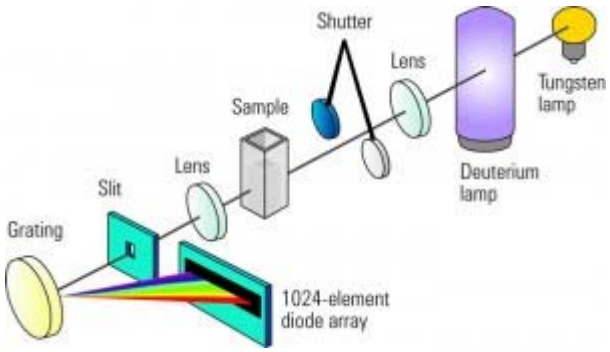

Fig 2.4: Single Beam UV-visible spectrophotometer

Double-beam UV-visible spectrophotometer

The light is split into two beams before it reaches the sample, in a double-beam spectrophotometer. In which one beam is used as the reference beam; the other which passes through the sample. The reference beam intensity is taken as 100% transmission (0% absorbance), and measurement displayed is the ratio of two beam intensities [50-51].

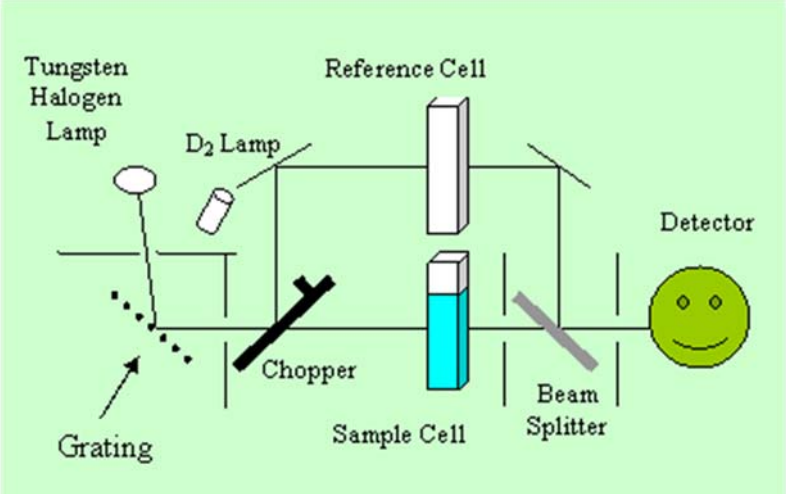

Fig 2.5: Double Beam UV- visible Spectrophotometer

Optical transmittance of Cu-doped PbS thin films as a function of wavelength in the near visible regions was measured using a SHIMADZU UV- VIS spectrophotometer (model: UV-2600/2700). Optical band gap of films was determined by using above procedure.

CHAPTER 3
CHARACTERIZATION OF Cu-DOPED PbS THIN FILMS

This chapter deals with the detailed characterization of undoped and Cu-doped PbS thin films grown by the CBD process as discussed in the previous chapter. In particular, this chapter presents the effects of copper doping on the evolution of crystal structural, surface microstructure and optical properties of the CBD PbS thin films.

Evolution of properties of undoped and Cu-doped PbS thin films

Thickness of a film is an important parameter for the quality performance in any photovoltaic (PV) device. It has been demonstrated that by depositing thin films for different deposition times photosensitive PbS thin films can be obtained with a thickness of up to ~300 nm, having p-type conductivity and associated with the cubic crystalline structure (galena) [28]. As far as PV is concerned, the thickness plays an important role in the absorption of photons. The generation of electron hole pair depends on the absorbed photons. As mentioned above, for thicknesses above 200 nm, more recombination occurs because the diffusion length of the minority carriers of PbS thin films is about 200 nm. Hence for thicker films, although photon is absorbed efficiently, the generated electron-hole pairs are not effectively dissociated and collected owing to the recombination in the absorber layer itself.

In this work, undoped and Cu-doped PbS thin films were prepared for different deposition times and copper concentration at a bath temperature of 60 ºC to examine their properties and to find the most suitable growth time for the PV devices. It was found that no film without Cu doping could be deposited for a time duration less than 5 min, although the same could be prepared for the PbS films doped with Cu of entire concentration range, i.e. 1 to 20 mol%. The evolution of film properties with the deposition time was investigated by XRD, SEM and UV visible spectroscopy.

3.1 Evolution of crystal structure

Figure 3.1 shows the typical XRD patterns of undoped PbS thin films grown on the glass substrate at 60 ºC for different deposition times ranging from 5 to 30 min. In the XRD patterns of the 5 and 10 min samples, only a broad hump in the range of 20° - 35° was observed that corresponded to the amorphous nature of the film and the glass substrate. As the deposition time was increased, there was evolution of multiple peaks indicating polycrystallinity of the

films. For the 30 min sample, the XRD pattern was characterized by six sharp Bragg peaks at 25.96º, 30.07º, 43.05º, 50.97º, 53.41º and 70.96º. These peaks were identified with the planes corresponding to the (111), (200), (220), (311), (222), and (420) planes of the PbS cubic phase, consistent with reference data [JCDPS 05 0592]. The quantitative variation in the peak intensity and the FWHM was estimated from Lorentzian fit to the highest intensity peak, i.e., the one corresponding to the (200) plane. It was observed that the peak intensity increased and the FWHM of the peaks decreased (from 0.2750° to 0.1838°) when the deposition increased from 20 to 30 min.

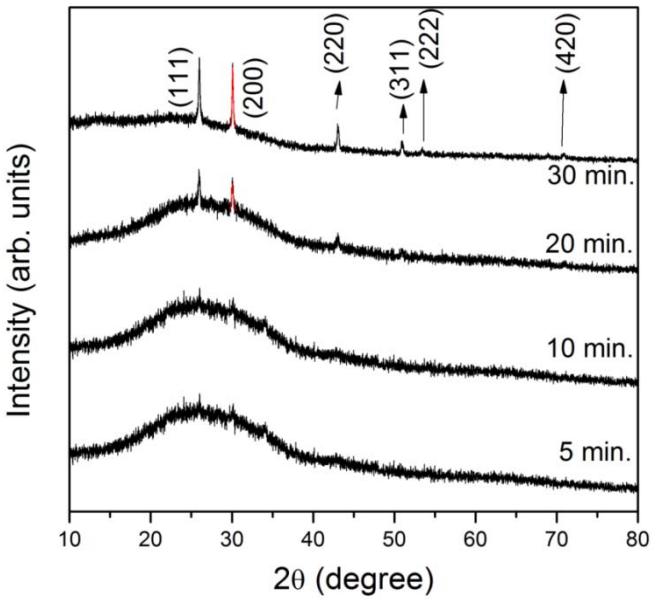

Fig. 3.1: Typical XRD patterns of the undoped PbS thin films grown on glass substrates at a bath temperature of 60 ºC for different deposition times.

The crystallite size (t_c) of the films was determined using Scherrer formula $t_c = \frac{0.9\lambda}{\beta\, Cos\theta}$ where λ is the wavelength of X-ray diffraction (1.54Å), β is the FWHM of the peak and 2θ is the Bragg's angle [92]. The average crystallite size for the thin films of deposition time of 20 and 30 min was found to be50 to 60 nm, respectively.

Figures 3.2 - 3.6 show typical XRD patterns of films grown at a bath temperature of 60 ºC for different deposition times with varying Cu concentration of 1, 2, 5, 10 and 20 mol%, respectively. In contrast to the undoped films, it was possible to deposit doped films for time duration as small as 2 min. The XRD patterns for the 2 min sample for all doping concentrations

showed a single peak at around 35° corresponding to Cu-S phase (Monoclinic Cu_7S_4, JCPDS file: 00-023-0958). It will be shown in the following pages (Section 3.2) that this phase is primarily responsible for development of a continuous film and provides a very distinct microstructure to the films. As the deposition time was increased, this peak disappeared and multiple peaks corresponding to various planes of Cubic PbS appeared in the patterns. Quantitative analysis based on Lorentzian fit to the (002) peak, the highest intensity peak, revealed that the intensity gradually increased while the FWHM of the peak decreased as the deposition time was increased, suggesting improved crystallinity with for higher deposition time. The variation of the peak intensity and the FWHM with deposition time for the doped and the undoped film is summarized in **Fig. 3.7**. For instance, in the 1% Cu-doped PbS films, the FWHM decreased from 0.3223° for 5 min of deposition to 0.1435° for 30 min of deposition time.

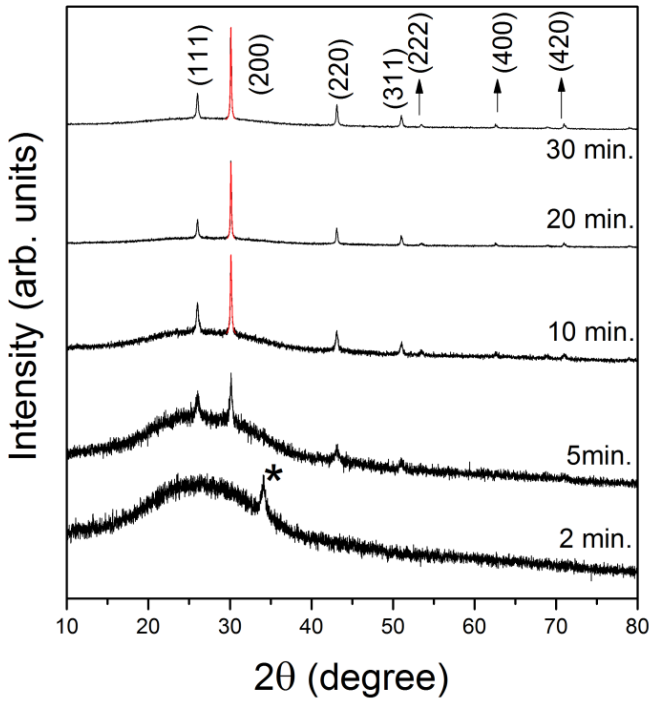

Fig. 3.2: Typical XRD pattern of 1% Cu doped PbS thin films grown on glass substrate at a bath temperature of 60 ºC for different deposition times. The asterisk (*) in the 2 min sample indicate that the initial phase formed in the film correspond to Cu_7S_4 phase.

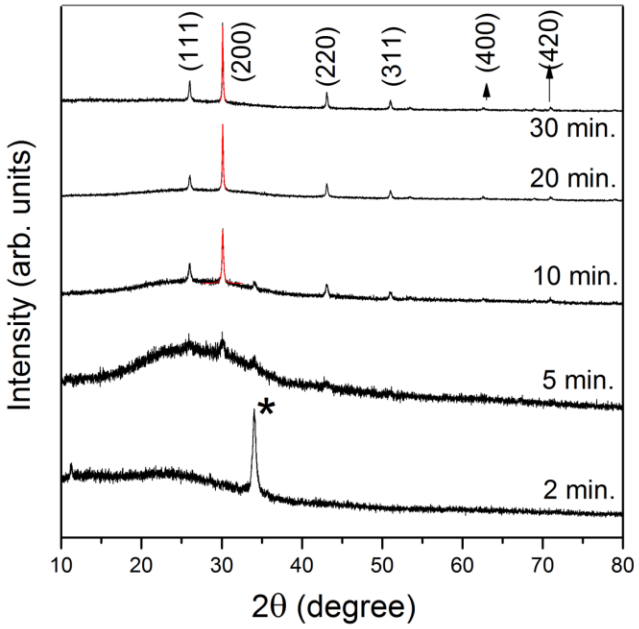

Fig. 3.3: Typical XRD pattern of 2% Cu doped PbS thin films grown on glass substrate at a bath temperature of 60 ºC for different deposition times. The asterisk (*) in the 2 min sample indicate that the initial phase formed in the film correspond to Cu_7S_4 phase.

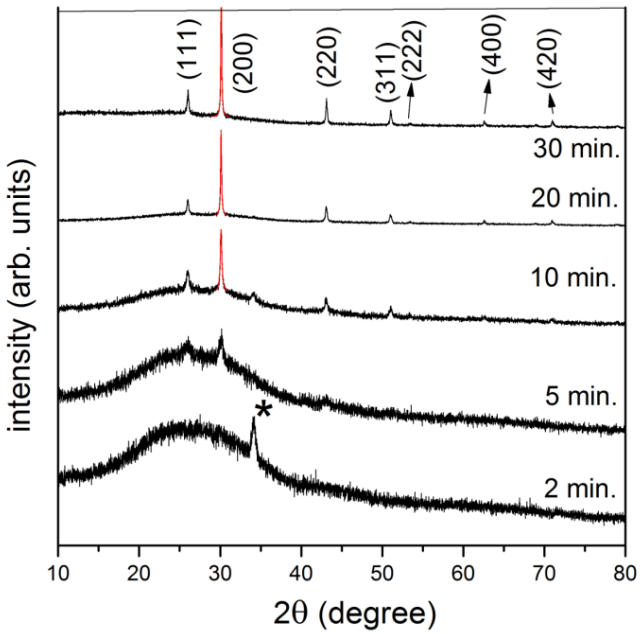

Fig. 3.4: Typical XRD pattern of 5% Cu doped PbS thin films grown on glass substrate at a bath temperature of 60 ºC for different deposition times. The asterisk (*) in the 2 min sample indicate that the initial phase formed in the film correspond to Cu_7S_4 phase.

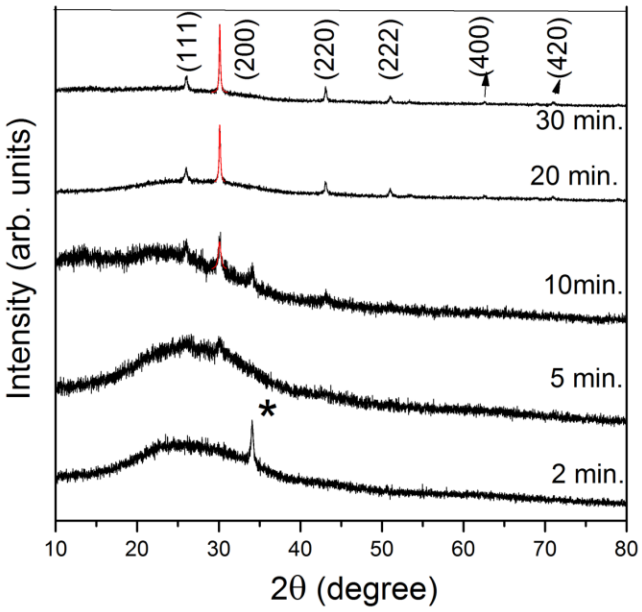

Fig. 3.5: Typical XRD pattern of 10% Cu doped PbS thin films grown on glass substrate at a bath temperature of 60 ºC for different deposition times. The asterisk (*) in the 2 min sample indicate that the initial phase formed in the film correspond to Cu_7S_4 phase.

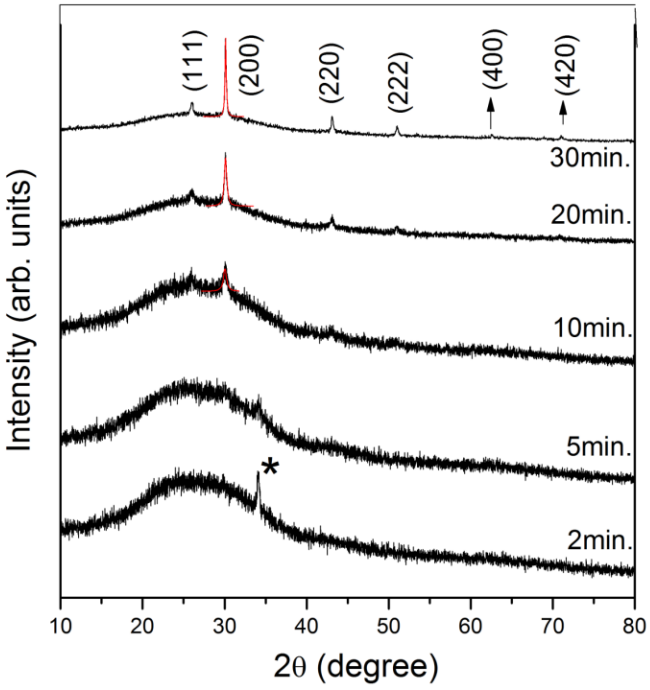

Fig. 3.6: Typical XRD pattern of 20% Cu doped PbS thin films grown on glass substrate at a bath temperature of 60 ºC for different deposition times. The asterisk (*) in the 2 min sample indicate that the initial phase formed in the film correspond to Cu_7S_4 phase.

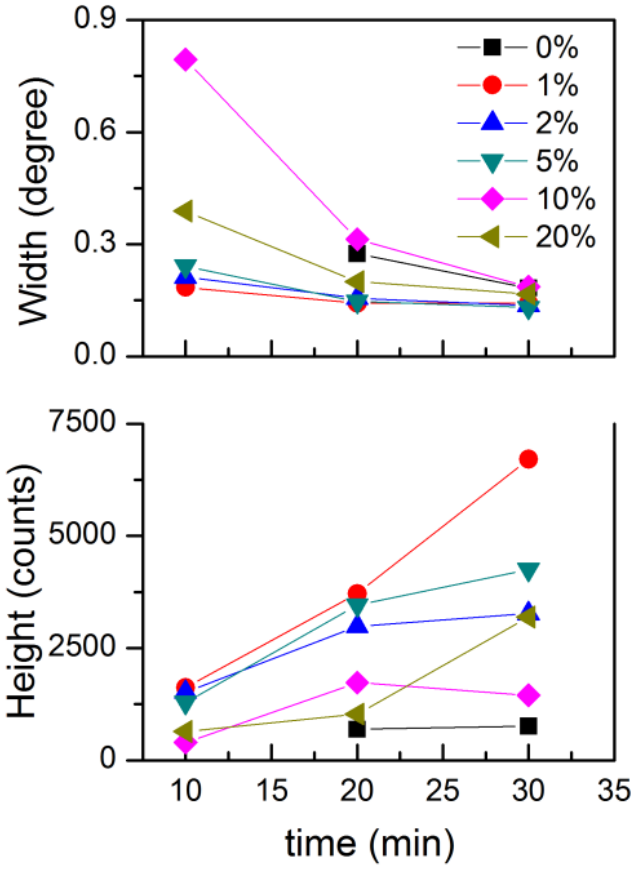

Fig. 3.7: Variation of the peak intensity and the FWHM with deposition time for the undoped and Cu-doped PbS thin films.

3.2 Doping controlled evolution of surface microstructure

Analysis of the XRD patterns of the undoped and Cu-doped PbS thin films showed that the films deposited for 30 min were well-crystallized characterized by multiple sharp Bragg peaks. Considering that a densely packed layer is a prerequisite for use as an absorber layer, a detailed microstructural investigation of the films was carried out. **Figure 3.8** shows the surface microstructure of the films deposited at a bath temperature 60 °C for duration of 30 min and whose XRD patterns have been presented in the previous section. The SEM image for the undoped film showed that the film is discontinuous with separated but well-developed crystallites. The crystallites are faceted and have a uniform distribution of size. However, a continuous film with a very contrasting microstructure was obtained when films were doped with Cu with even an amount as small as 1%.

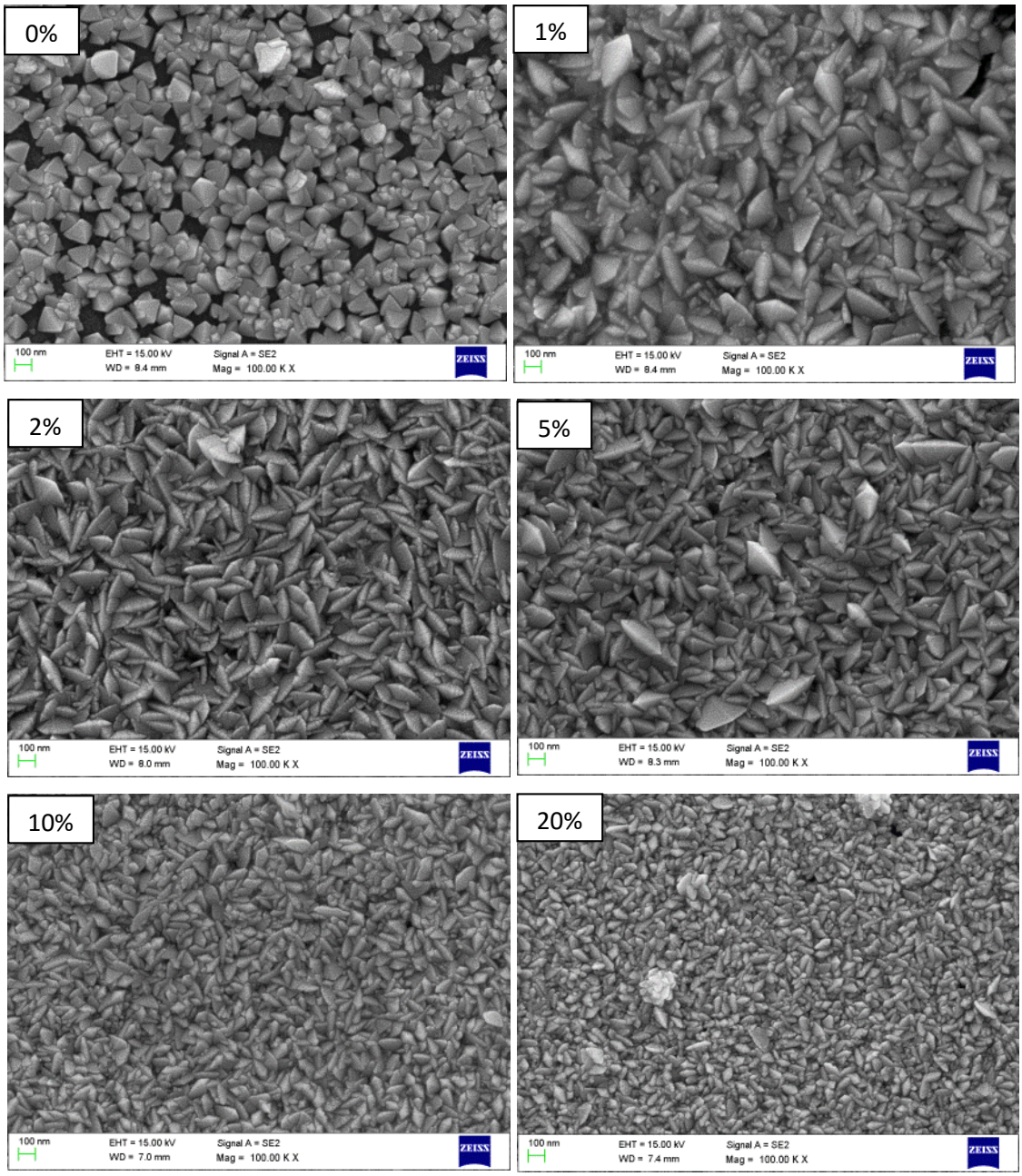

Fig. 3.8: Representative SEM images of undoped and Cu doped PbS thin films prepared at 60 ºC for 30 minutes. All images were taken at same magnification (10^5 X)

The doped films showed a continuous film with surface covered by crystallites whose size and shape continuously decreased with the increase in Cu concentration. For the 1% doped films, a bimodal surface structure was observed. A majority of the crystallites were elongated with a high aspect ratio, and the others were of small dimensions and having an aspect ratio of nearly 1:1. This non-uniformity disappeared as the Cu amount in the films was increased. For

instance, the surface was found to be covered by crystallites of similar types in the 10 and 20% Cu-doped PbS films. These crystallites had similar aspect ratio and similar dimensions. It is interesting to note, however, that the dimension of the crystallites continuously decreased. The sharp contrasts in the surface microstructure of the films are thought to arise as a consequence of the doping and the doping concentration. The effects of thickness is ruled out based on the fact that all films were grown for the same duration and cross-sectional images of the films showed that thickness of all films was about 200 nm. In order to ascertain the origin of the microstructural anomaly films of smaller durations were grown and detailed characterization was carried out.

Figure 3.9 shows the evolution of surface microstructure of the undoped PbS thin films prepared at 60º C for different deposition times. It depicts a picture of a discontinuous film with surface covered by irregularly shaped three dimensional crystallites, whose number and size changed with deposition time. However, despite a long deposition time of 30 min, the film was still discontinuous.

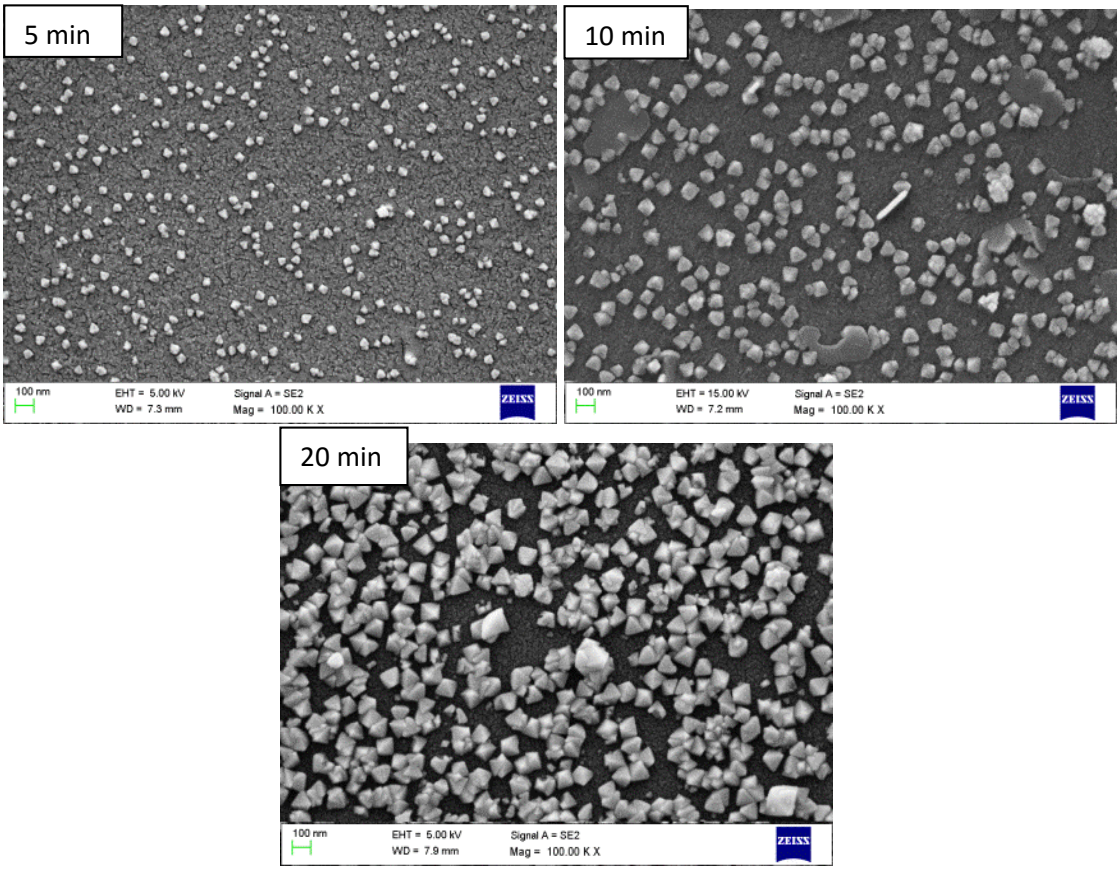

Fig. 3.9: Typical SEM images of undoped PbS thin films for different durations.

Figure 3.10 shows the variation in the number of particulates covering the film surface of area 3 μm × 2 μm. It shows that the number of particulates marginally decreased as the deposition time was increased from 5 to 10 min, although the area covered by the particulates increased. This indicates that although new particulates were heterogeneously nucleated existing particulates coalesced. However, as deposition time increased, the number of particulates and the %area covered increased and stabilized around 20 min. It is worth noting here that the size and shape of particulates are uniform at all stages of film growth.

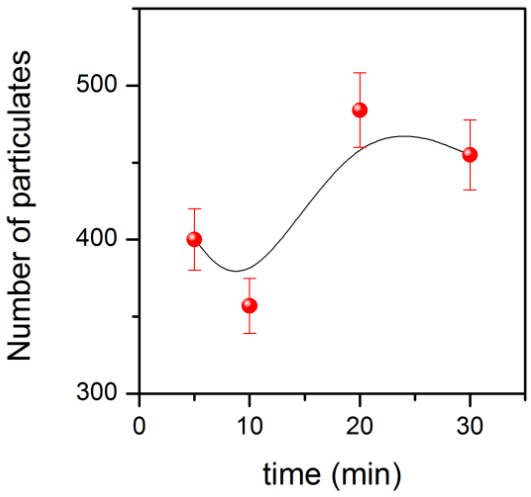

Fig. 3.10: Plot of variation of number of particulates with deposition time for the films grown at bath temperature 60º C.

Figure 3.11 shows the evolution of surface microstructure with deposition for the 1% Cu-doped PbS thin films. In contrast to the undoped films, the SEM images show a continuous film at all stages of film growth. The substrate surface was uniformly coated with a thin layer for after 2 min of deposition. On this surface, proceeded the further growth of the films that eventually (after 30 min of deposition) resulted in a bimodal distribution of crystallites. At all stages, it was found that the surface was covered with two types of crystallites: a majority of them having elongated structure and other of smaller dimensions with aspect ratio of about 1:1. For the 2, 5, 10 and 20% Cu-doped films, the evolution of microstructure has been presented in **Figs. 3.12** to **3. 15** respectively. It was found that for all doping concentration, there was a uniform coating after 2 min, on which the further growth of the films proceeded. This coating is thought to be critical that determined the eventual surface structure.

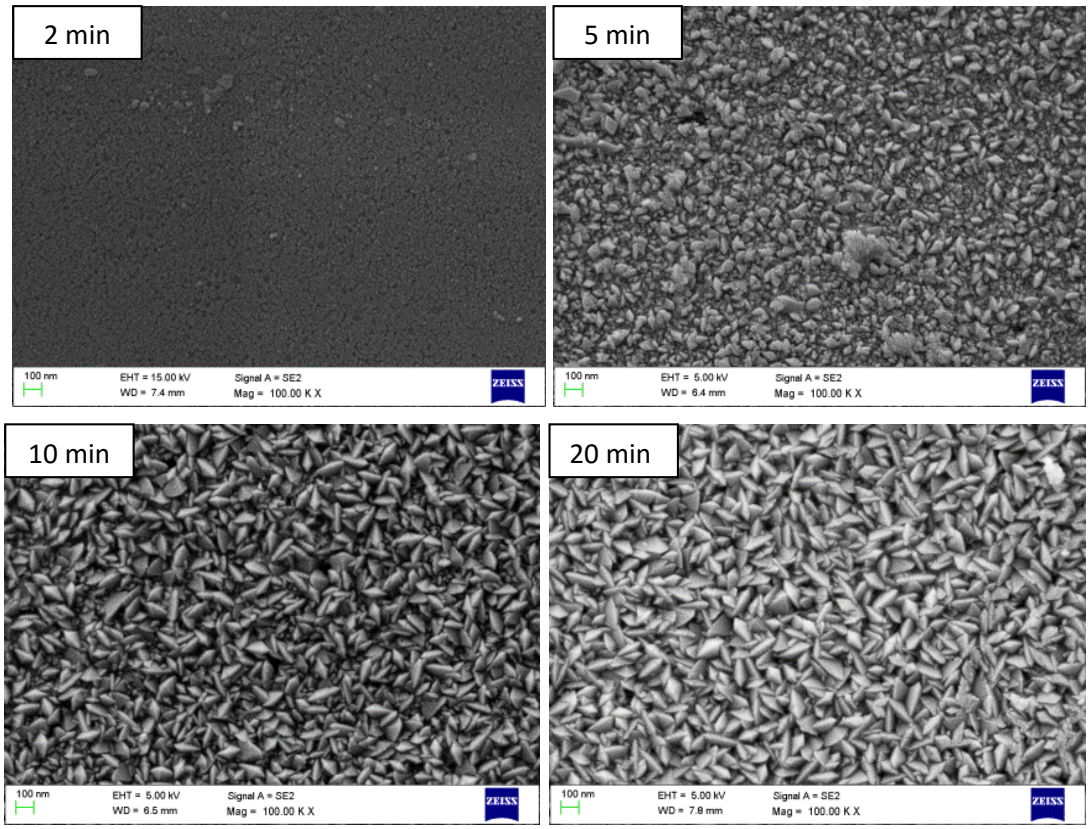

Fig. 3.11: SEM images of 1% Cu doped PbS thin films prepared for different durations.

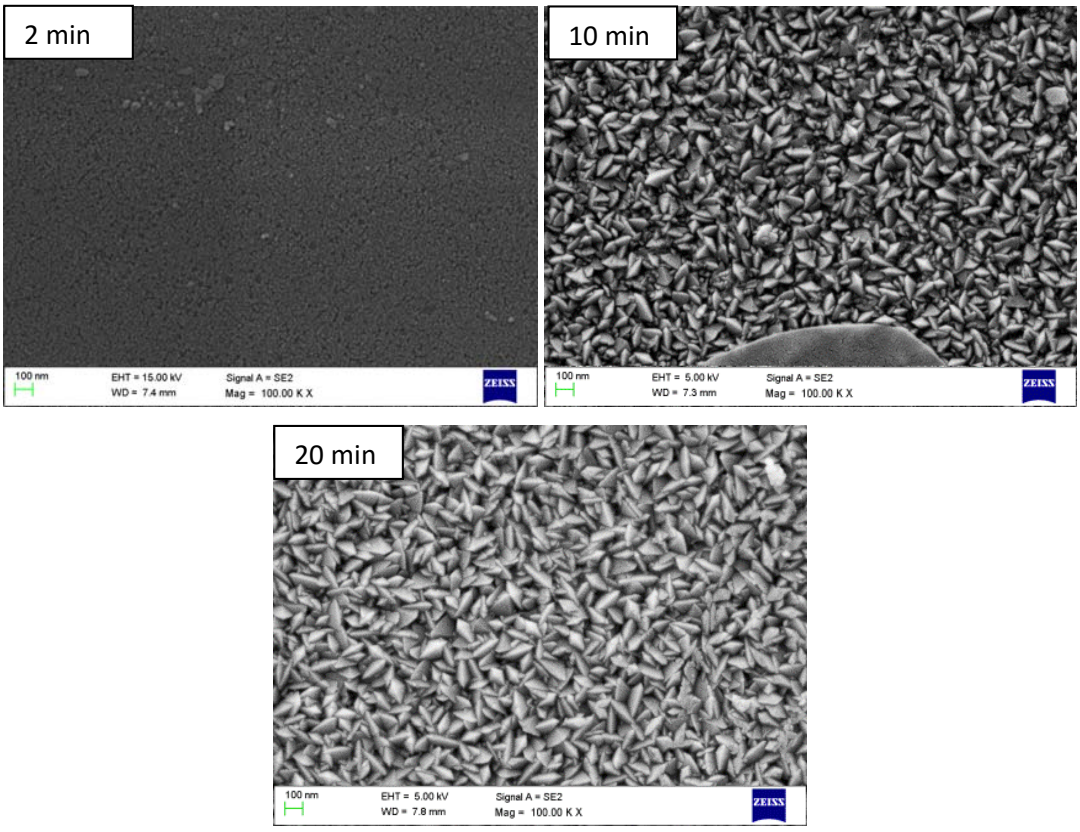

Fig. 3.12: SEM images of 2% Cu doped PbS thin films prepared for different durations.

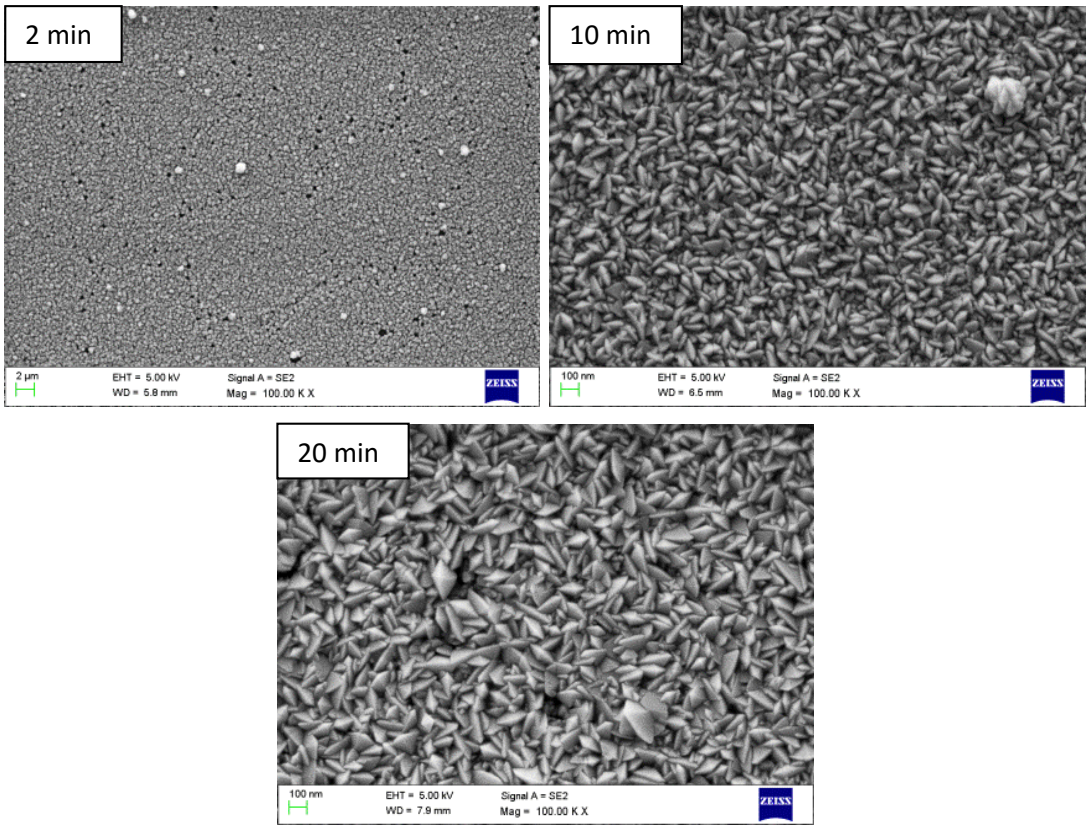

Fig. 3.13: SEM images of 5% Cu doped PbS thin films prepared for different durations.

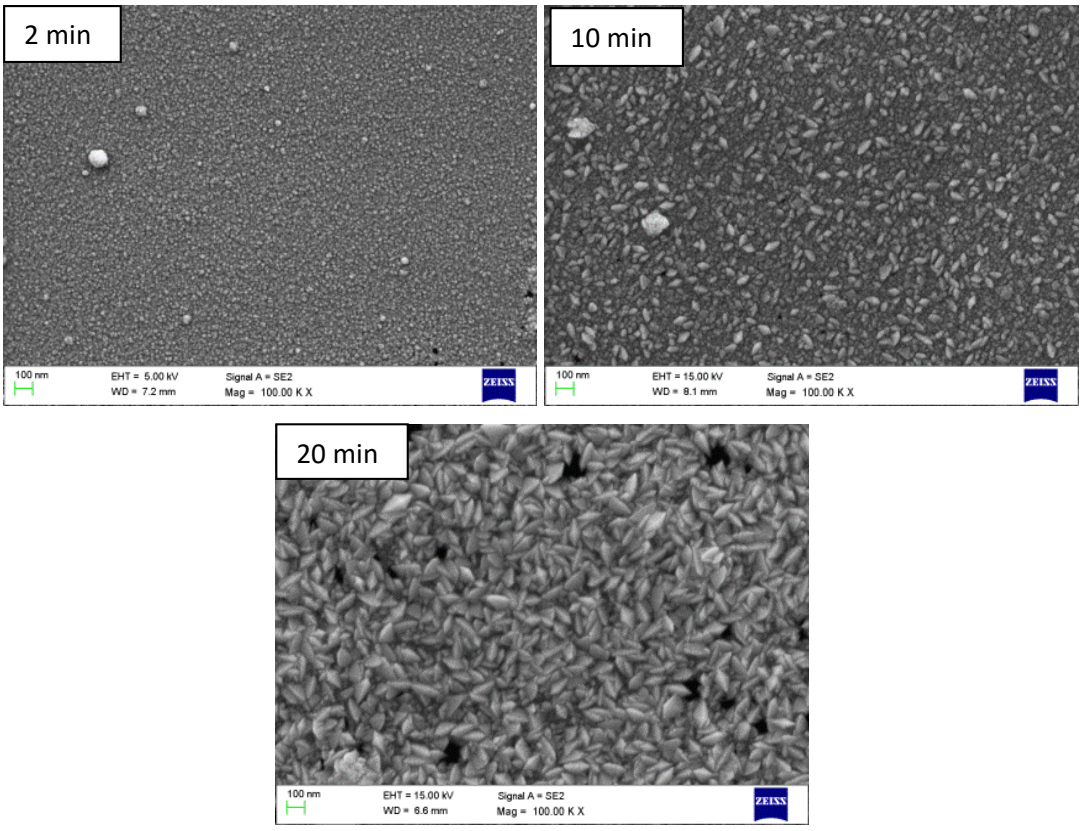

Fig. 3.14: SEM images of 2% Cu doped PbS thin films prepared for different durations.

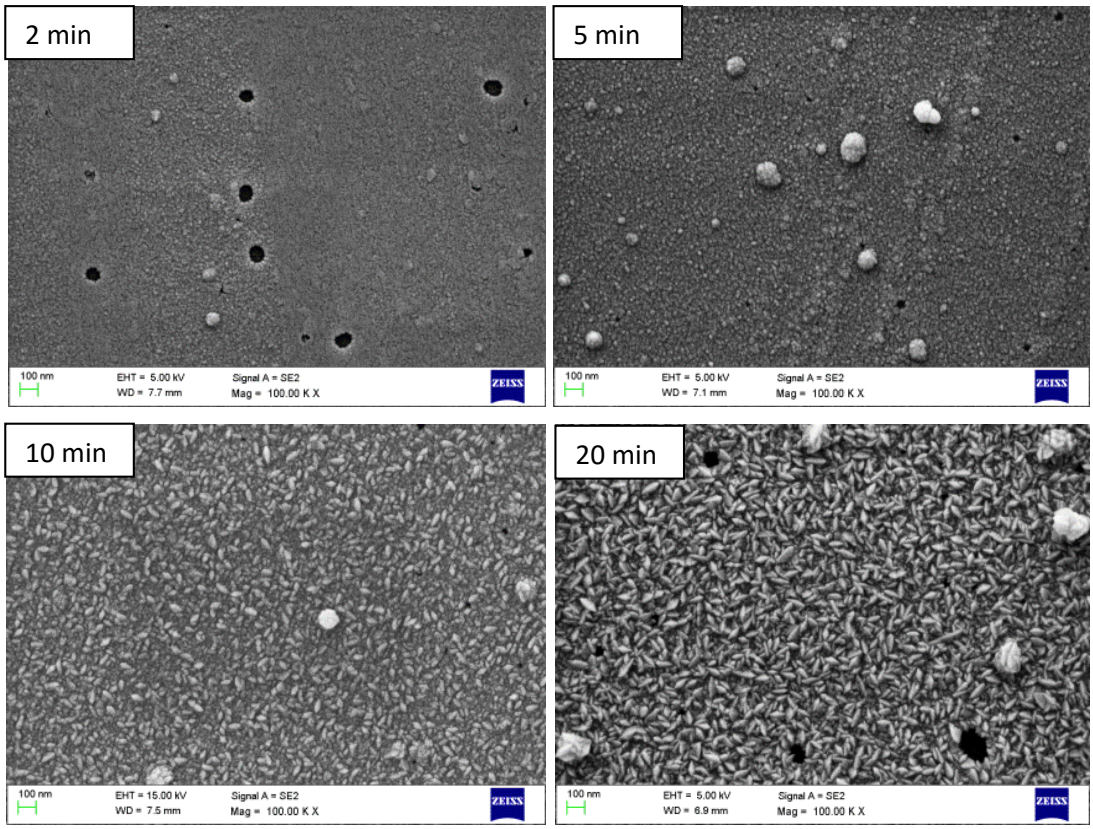

Fig. 3.15: SEM images of 2% Cu doped PbS thin films prepared for different durations.

As the **Figs. 3.11 to 3.15** indicate, the doping determined the eventual surface microstructure of the films. As mentioned before, the doping controlled growth of the film at the initial stage (i.e., 2 min deposition sample) is critical to the subsequent development of the surface features. From the XRD analysis of the 2 min samples, it was found that the initial layer is devoid of Pb and contained only Cu and S leading to the formation of the phase Cu_7S_4. This layer is thought to be the nucleating layer, on which occurred the further growth of the films. The release of Pb ions and subsequent reaction with S follows the release and reactions between Cu and S. Based on this argument, the contrasting surface features of the undoped samples can be understood. It may also explain why there could be no undoped film for a deposition time less than 5 min.

3.3 Effect of Cu doping on optical properties of the PbS thin films

As discussed in Chapter 1, optical properties, namely band gap and the absorption of the semiconductor layer largely govern its suitability for the solar cell applications. While the bulk PbS has a very small band gap of ~0.41 eV, it can be increased to 1 - 1.5 eV in the case of PbS quantum dots, leveraging the benefits of quantum confinement effect. Recently, PbS

quantum dot based solar cells have drawn significant interest. However, fabrication, surface passivation of the quantum dots, and issues of their light and air stability have posed serious concerns on scalable production of these devices. It is believed that Cu-doping may help increasing the band gap, all the while maintaining the simplicity of the deposition technique.

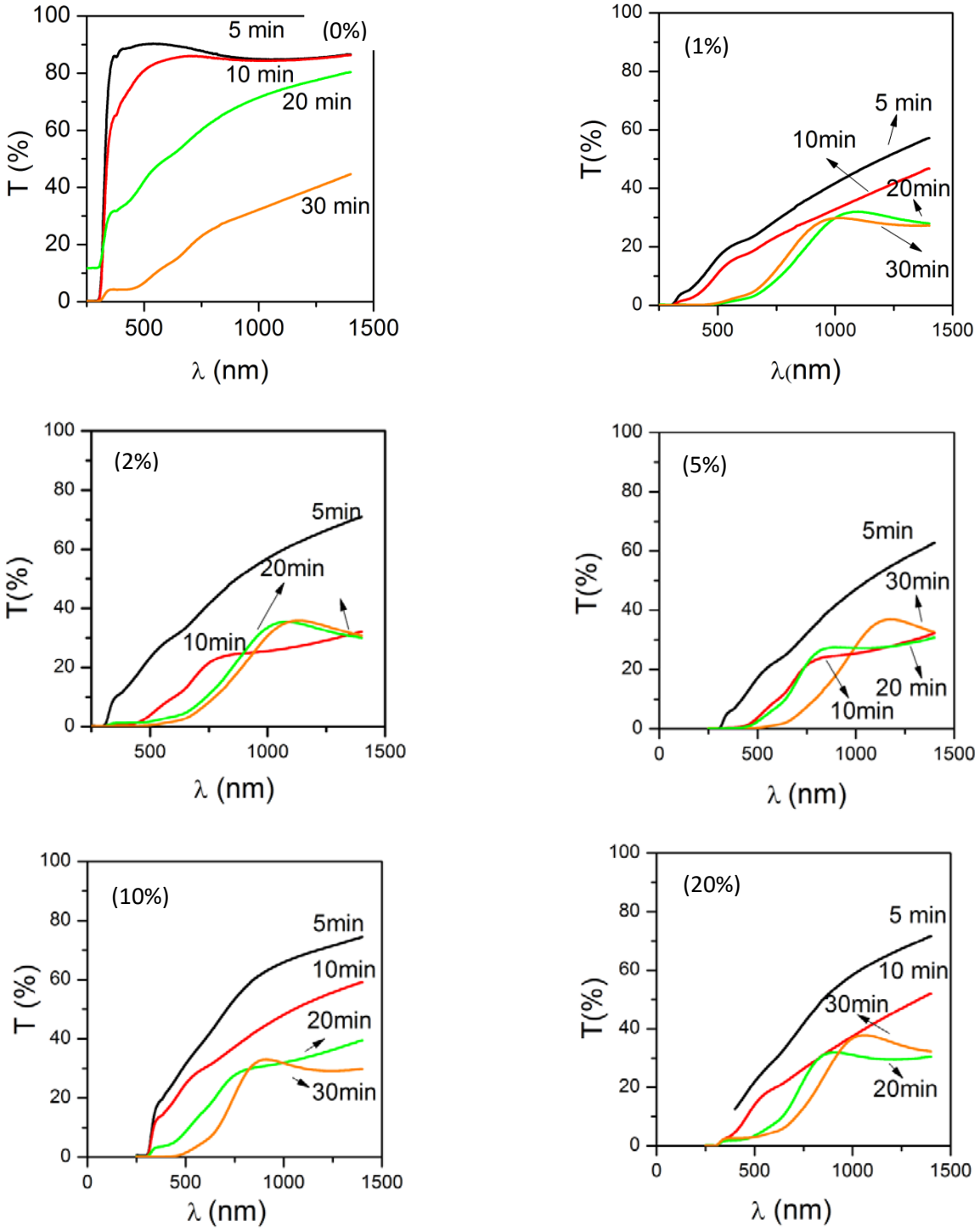

Fig. 3.16: Wavelength dependence of transmittance of undoped and doped PbS thin films deposited for different durations.

Typical transmittance spectra for PbS thin films obtained for different deposition times are presented in **Figure 3.16.** Note that correction due to the glass substrates has not been made. For the undoped films, the transmittance remained relatively higher compared to the doped samples because of the discontinuous nature of the undoped films. However, with increase in deposition time, the transmittance decreased gradually due to the increased surface coverage of the glass substrates. Thus, we have not made any attempt to estimate the band gap from these curves as that would incur large errors. For all the doped films, the transmittance gradually decreased with increasing deposition time due to higher absorption of incident photons. Typically for the thicker films (i.e., deposition time of 30 min), the maximum transmittance in the wavelength range of 300 to 1400 nm remained less than 30 %. As mentioned in chapter 2, the band gap of the films was determined from the plots of $(\alpha h\nu)^2$ vs $h\nu$. The linear portion of the curves was extrapolated to the zero value of y-axis to determine the band gap. [50-51].

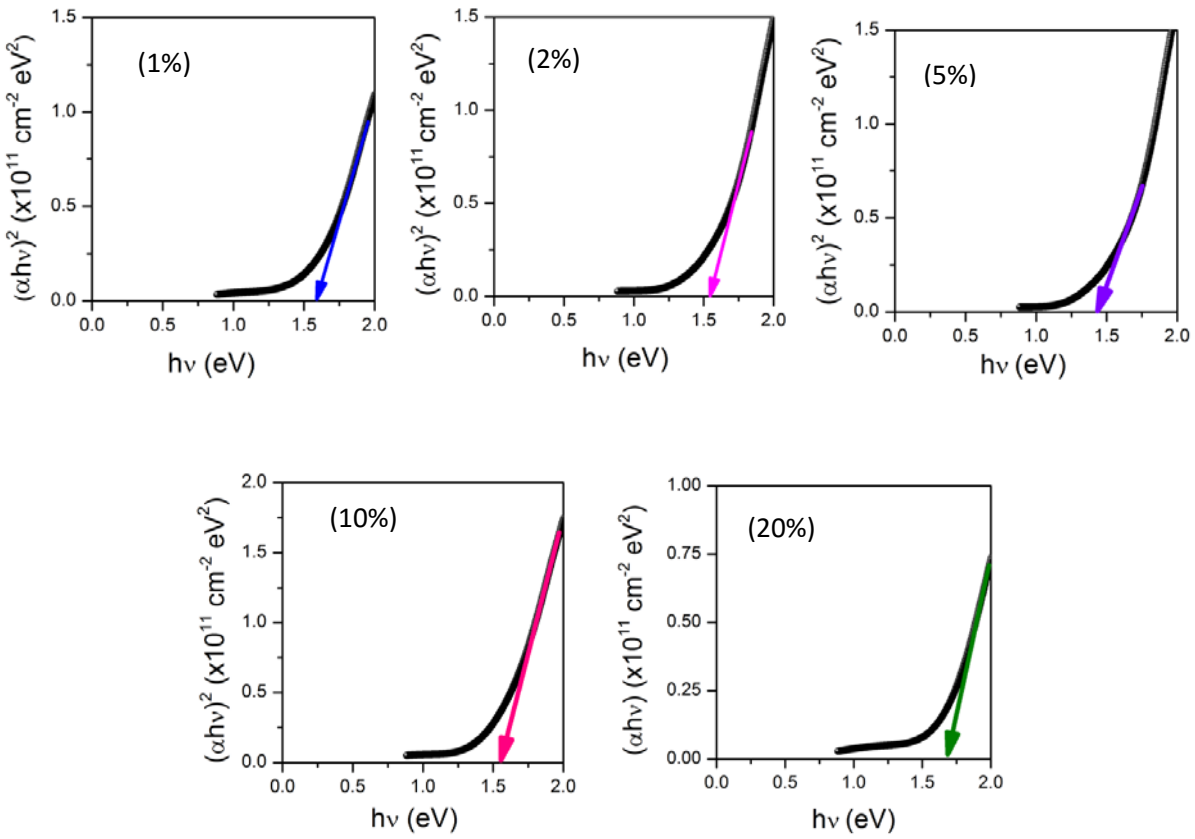

Fig. 3.17: Variation of $(\alpha h\nu)^2$ vs the photon energy $h\nu$ for the films deposited for 30 min.

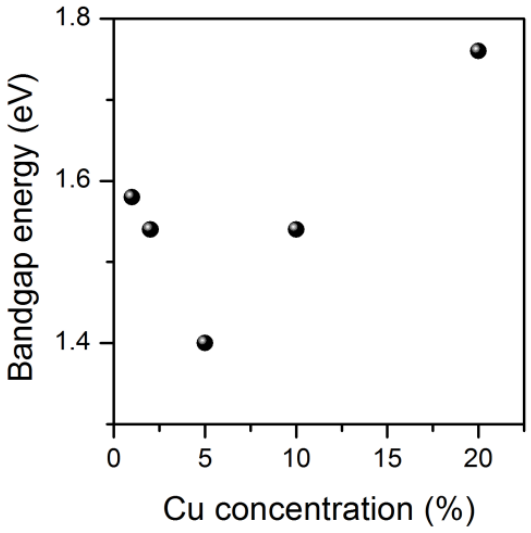

Fig. 3.18: Variation of the band gap of the Cu-doped PbS thin films (deposition time of 30 min) as a function of Cu concentration.

Figure 3.17 shows the variation of $(\alpha h\nu)^2$ vs the photon energy hν for the films deposited at 60 ºC for 30 min. A linear least-square fitting was carried out in the linear portion of the curves to determine the band gap. **Figure 3.18** shows the variation of the band gap of the Cu-doped PbS thin films (deposition time of 30 min) as a function of Cu concentration. For small concentration of Cu up to 5%, the band gap marginally decreased and then, continuously increased from about 1.40 eV for 5% Cu doping to about 1.76 eV for 20% Cu-doping. Based on these results, it is believed that Cu-doped PbS thin films grown by the CBD process can be a potential candidate for PV applications.

CONCLUSIONS AND FUTURE SCOPE

Cu-doped PbS thin films were grown on glass substrates by the chemical bath deposition (CBD) process. Since the control of process parameters is relatively easier, this technique has been traditionally used in deposition of thin films. Furthermore, it requires inexpensive setup and films can be deposited on large area. Thus, CBD technique has been a user friendly technique. Lead acetate, thiourea and copper chloride were used in aqueous solution as ion sources of Pb, S and Cu, respectively. All films were synthesized in a single step by dipping the substrates in the bath solution held at a temperature of 60 °C. The deposition time was varied from 2 to 30 min to investigate the evolution of the properties. The properties of resulting thin films were characterised by various techniques such as X- ray diffraction (XRD), field emission scanning electron microscope (FE- SEM) and UV-visible spectroscopy. It was found that for the undoped films, no deposition was possible up to a deposition time of 5 min. When the substrates were dipped for longer durations, the growth of the films proceeded from heterogeneous nucleation of crystallites followed by their coalescence. The films were found to be discontinuous for deposition times as long as 30 min. In contrast, the doped films showed a continuous film with surface covered by crystallites whose size and shape continuously decreased with the increase in Cu concentration. The continuous nature of the film is attributed to the formation of the initial layer of Cu_7S_4, as revealed from the XRD analysis, on which further growth of the films proceeded. For all the doped films, the transmittance gradually decreased with increasing deposition time due to higher absorption of incident photons. For small concentration of Cu up to 5%, the band gap marginally decreased and then, continuously increased from about 1.40 eV for 5% Cu doping to about 1.76 eV for 20% Cu-doping.

This work presents an interesting observation of doping controlled evolution of microstructure in the PbS thin films. A more detailed examination using Raman spectroscopy and high resolution transmission electron microscopy can reveal the dominant facets of the particulates of the undoped films and the phases at initial and final stages. Although it was not attempted to fabricate any solar cell using these p-type films as absorber layers, it is believed that Cu-doped PbS thin films grown by the CBD process can be a potential candidate for PV applications.

References

1. R. H. Bossert, C. J. J. Tool, J. A. M. van Roosmalen, C. H. M. Wentink, and M. J. M. de Vaan, “Thin-film solar cells, technology evaluation and perspectives,” Tech. Rep., 2000, http://citeseerx.ist.psu.edu/viewdoc/download?doi=10.1.1.196.7245&rep=rep1&type=pdf.
2. K. L. Chopra, “Thin Film Solar Cells,” Mc-Graw Hills (1983).
3. D. Smith, “Thin Film Deposition: Principles and Practice”, McGraw-Hill Professional (1995).
4. Z. Zhuang, X. Lu, Q. Peng and Y. Li, "A Facile “Dispersion–Decomposition” Route to Metal Sulfide Nano crystals," Chem. -Eur. J., **17**, 10445 (2011).
5. D. B. Mitzi, O. Gunawan, T. K. Todorov, K. Wang, S. Guha, “The Path Towards a High-Performance Solution-Processed Kesterite Solar Cell” Solar Energy Mater. Solar Cells, **95**, 1421-1436 (2011).
6. L. Yu, Y. Lv, G. Chen, X. Zhang, Y Zeng, H. Huang and Y. Feng, “A Generally Synthetic Route to Semiconducting Metal Sulfide Nanocrystals by using Corresponding Metal Powder and Cysteine As Metallic and Sulphuric Sources, respectively,” Inorg. Chim. Acta **376**, 659 (2011).
7. J. S. Steckel, J.P. Zimmer, S.Coe- Sullivan, N.E. Stott. V. Bulovic and M.G. Bawendi, “Blue Luminescence from (CdS) ZnS Core-Shell Nanocrystals”, Angew. Chem. Int. Ed, **43**, 2154(2004).
8. A.U. Ubale, A. R. Junghare, N. A. Wadibhasme, A. S. Daryapurkar, R. B. Mankar, V. S. Sangawar, “Thickness Dependent Structural, Electrical and Optical Properties of Chemically Deposited Nanoparticles PbS Thin Films” Turk J Phys. **31** (2007) , 279 – 286.
9. U. Jadhav, M. Shinde, S. Patel and R. Patil, "Structural, Optical and Electrical Properties of Nanocrystalline Cadmium Sulphide Thin Films Deposited by Novel Chemical Route," Indian J. Pure App. Phy., **52**, 39 (2014).
10. K. P. Bhandari, P. J. Roland, H. Mahabaduge, N. O. Haugen, C. R. Grice, S. Jeong, T. Dykstra, J. Gao and R. J. Ellingson, "Thin Film Solar Cells Based on The Heterojunction of Colloidal PbS Quantum Dots with CdS," Solar Energy Mater. Solar Cells, **117**, 476 (2013).

11. I. Pop, C. Nascu, V. Ionescu, E. Indrea, and I. Bratu, “Structural and Optical Properties of PbS Thin Films Obtained by Chemical Deposition”, Thin Solid Films **307,** 240 (1997).
12. N. Mott, “Conduction in Non-Crystalline Materials”, Claredon Press, Oxford, 1987.
13. O.A. Gudaev, V.K. Malinovsky, E.E. Paul, V.A. Treshikhin, “The influence of photoexcitation level on the process of charge transfer in polycrystalline PbS films”, Solid State Comm. **72**, 791 (1989).
14. G.H. Blount, P.J. Schreiber, D.K. Smith, R.T. Tamada, “Photoconductive properties of chemically deposited PbS with dielectric overcoatings” J. Appl. Phys. **44**,978 (1973).
15. S.M. Pawar, B.S. Pawar, J.H. Kim, Oh-Shim Joo and C.D. Lokhande, “Recent Status of Chemical Bath Deposited Metal Chalcogenide and Metal Oxide Thin Films” Current Appl. Phys. **11**, 120 (2011).
16. S. Seghaier, N. Kamoun, R. Brini, and A.B. Amara, “Structural and Optical Properties of PbS Thin Films Deposited by Chemical Bath Deposition Technique”, Mater. Chem. Phys. **97**, 71 (2006).
17. G.P. Kothiyal, B. Gosh, R.Y. Deshpande, “Effect of morphological structure on photosensitivity of chemically deposited PbS thin films” J. Phys. D: Appl. Phys **13**, 869 (1980).
18. H. Pathan and C. Lokhande, "Deposition of Metal Chalcogenide Thin Films by Successive Ionic Layer Adsorption and Reaction (SILAR) Method," Bull. Mater. Sci., **27** 85 (2004)
19. P.K. Nair et al., “Semiconductor Thin Films by Chemical Bath Deposition for Solar Energy Related Applications” Solar Energy Mater. Solar Cells 52, 313 (1998)
20. G. Hodes, “Chemical Solution Deposition of Semiconductor Thin Films”, Marcel Dekker, (2003).
21. K C Preetha, K V Murali, A J Ragina, K Deepa, A C Dhanyal and T L Remadevi, “The Role of Cationic Precursors in Structural, Morphological and Optical Properties of PbS Thin Films” IOP Conf. Ser.: Mater. Sci. Eng. **43** 012009 (2013).
22. F.Göde, E.Güneri, F.M. Emen, V. Emir Kafadar, S. Ünlü, “Synthesis, Structural, Optical, Electrical and Thermo Luminescence Properties of Chemically Deposited PbS Thin Films” J. Luminescence, **147,** 41 (2014).
23. P K Nair, V M Garcia, A B Hernandez and M T S Nair, “Photo Accelerated Chemical Deposition of PbS Thin Films: Novel Applications in Decorative Coatings and Imaging Techniques” J. Phys. D: Appl. Phys. **24**, 1466 (1991).

24. L. Raniero, C.L. Ferreira , L.R. Cruz , A.L. Pinto , R.M.P. Alves, “Photoconductivity Activation in PbS Thin Films Grown at Room Temperature by Chemical Bath Deposition” Physica B **405**, 1283 (2010).
25. Barış Altıokka, Mevlana Celalettin Baykul, Mehmet Rıza Altıokka, “Some Physical Effects of Reaction Rate on PbS Thin Films Obtained By Chemical Bath Deposition” J. Crystal Growth **384**, 50–54 (2013).
26. Ileana Pop, Cristina Nascu, Vioteta Ionescu, E. Indrea I. Bratu, “Structural and Optical Properties of PbS Thin Films Obtained by Chemical Deposition” Thin Solid Films, **307**, 240-244 (1997).
27. J.J. Valenzuela-J´aureguia, R. Ram´ırez-Bona, A. Mendoza-Galva´na, M. Sotelo-Lermab, “Optical Properties of PbS Thin Films Chemically Deposited at Different Temperatures” Thin Solid Films, **441**,104 (2003).
28. M.M. Abbas, A. Ab-M. Shehab, N-A. Hassan, A-K. Al-Samuraee, “Effect of Temperature and Deposition Time on the Optical Properties of Chemically Deposited Nanostructure PbS Thin Films” Thin Solid Films **519**, 4917 (2011).
29. J.A. García-Valenzuela, M.R. Baez-Gaxiola, M. Sotelo-Lerma, “Chemical Bath Deposition of PbS Thin Films on Float Glass Substrates using a Pb(CH3COO)2–NaOH–(NH2)2CS–N(CH2CH2OH)3–CH3CH2OH Definite Aqueous System and their Structural, Optical, and Electrical/Photoelectrical Characterization” Thin Solid Films **534**, 126 (2013).
30. T. Tohidi, K. Jamshidi-Ghaleh, Namdhar and R. Abdi- Ghaleh, “ Comparative Studies On the Structural, Morphological, Optical and Electrical Properties of Nanocrystalline PbS Thin Films Grown by Chemical Bath Deposition Using Two Different Bath Composition,” Mater. Sci. Semiconductor Processing, **11**, 100 (2013).
31. R.S. Patil, H. M. Pathan, T.P. Gujar and C.D. Lokhande, “Characterization of Chemically Deposited Nano crystalline PbS Thin Films”, J. Mater. Sci. **41**, 5723 (2006).
32. A.S. Obaid, M.A. Mahdi, Z. Hassan and M. Bououdina, “Characterization of Nanocrystalline PbS Thin Films Prepared using Microwave-Assisted Chemical Bath Deposition,” Mater. Sci. Semiconducting Processing, **15**, 564 (2012).
33. Zongbo Huang, Xiaoping Zou n, Hongquan Zhou, “A Strategy to Achieve Superior Photocurrent by Cu-doped Quantum Dot Sensitized Solar Cells” Mater. Lett. **95**, 139 (2013).

34. R. Palomino-Merino, O. Portillo-Moreno, J. C. Flores-García, J. Hernández-Tecorralco, J. Martínez-Juárez, A. Moran-Torres, E. Rubio-Rosas, G. Hernández-Téllez, R. Gutiérrez-Pérez, and L. A. Chaltel-Lima, "PbS Nanostructured Thin Films by In Situ Cu-Doping" Nanoscience and Nanotechnology **14**, 5408–5414, 2014
35. V. Popescu, H. I. Nas-cu and E. Darvasi," Optical Properties of PbS-CdS Multilayers and Mixed Thin Films Deposited on Glass Substrate by Spray Pyrolysis," J. Optoele. Adv. Mater., **8**, 118 (2006).
36. S. Prabaha, N. Suryanaranyanan, K. Rajasekar and S.Srikanth, "Lead Selenide Thin Films from Vaccum Evaporation Method - Structural and Optical Properties," Chalcogenide Lett. **6**, 204 (2009).
37. M. Farady, A. I. Hochbaum, J.Goldberger, M.Zhang and P.Tang, "Synthesis and Thermoelectrical Characterization of Lead Chalcogenide Nanowires," Advanced Materials, **19**, 3047 (2007).
38. J. Aguilar-Hernandez," Photoluminescence and Structural Properties of Cadmium Sulfide Thin Films Grown by Different Techniques," Semicond. Sci. Technol., **18**, 111 (2003).
39. E. Pentia, L. Pintilie, I. Matei, T. Botila and E. Ozbay," Chemically Prepared Nanocrystalline PbS Thin Films," J. of Optoele. Advanced Mater, **3**, 525 (2001).
40. B. D. Cullity, "Elements of X-ray diffraction," 2nd Edn., Addison-Wesley, Massachusetts, (1978).
41. I. M. Watt, "The principles and practice of electron microscopy," Cambridge University Press, Cambridge (1983).
42. P. J. Goodhew, J. Humphreys and R. Beanland, "Electron Microscopy and Analysis," Taylor Francis, London, (2000).
43. K. S. Birdi, "Scanning Probe Microscopes: Applications in Science and Technology," CRC Press, Boca Raton (2003).
44. E. Meyer, H. J. Hug and R. Bennewitz, "Scanning Probe Microscopy: The Lab on a Tip," Springer- Verlag Berlin (2004).
45. S. Morita, R. Wiesendanger and E. Meyer, "Noncontact Atomic Force Microscopy," Springer: Berlin (2002).
46. A. Mehta, "UV-Vis Spectroscopy- Limitations and Deviations of Beer- Lambert Law," Analytical Chemistry (2012).
47. P. Misra and M. A. Dubinskii, "Ultraviolet Spectroscopy and Uv- Lasers," New York, Marcel Dekker (2002).

48. B. W. Kempshall, L. A. Giannuzzi, B. I. Prenitzer, F. A. Stevie and S. X. Da, “Comparative Evaluation of Protective Coatings and Focused Ion Beam Chemical Vapor Deposition Processes,” J. Vacuum Sci. Technol. B **20**, 286 (2002).
49. O. Zelaya-Angel, J.J. Alvarado-Gil, R. Lozada-Morales, H. Varges and A. Ferreira da Silva, “Band-Gap Shift in CdS Semiconductor by Photo acoustic Spectroscopy: Evidence of a Cubic to Hexagonal Lattice Transition” Appl. Phys. Lett. **64**, 291 (1994).
50. M. Rusu, A. Rumberg, S. Schuler, S. Nishiwaki, R. Wurz, S.M. Babu, M. Dziedzina, C. Kelch, S. Siebentritt, R. Klenk, Th. Schedel-Niedrig and M.Ch. Lux-Steiner, “Optimisation of the CBD CdS Deposition Parameters for ZnO/CdS/CuGaSe Solar Cells,” J. Phys. Chem. Solids **64**,1849 (2003).